SACLANTCEN Conference Proceedings No. 17 Part 6

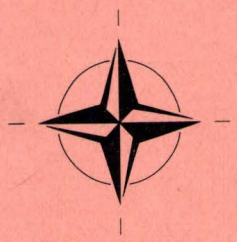

SACLANTCEN
Conference Proceedings No. 17

PART 6
MICRO-SCALE PHENOMENA

SACLANT ASW
RESEARCH CENTRE

OCEANIC ACOUSTIC MODELLING

Proceedings of a Conference held at SACLANTCEN
on 8-11 September 1975

Organized by

WOLFGANG BACHMANN and ROBERT BRUCE WILLIAMS

15 OCTOBER 1975

NORTH
ATLANTIC
TREATY
ORGANIZATION

VIALE SAN BARTOLOMEO 400
I - 19026 - LA SPEZIA, ITALY

Compiled and Published by

STI
SACLANTCEN

SACLANTCEN
CONFERENCE PROCEEDINGS NO. 17

NORTH ATLANTIC TREATY ORGANIZATION
SACLANT ASW Research Centre
Viale San Bartolomeo 400
I 19026 - La Spezia, Italy

OCEANIC ACOUSTIC MODELLING

Proceedings of a Conference held at SACLANTCEN
on 8-11 September 1975

In eight parts
Part 6: Micro-Scale Phenomena

Organized by
Wolfgang Bachmann and Robert Bruce Williams

15 October 1975

PAPERS PRESENTED AT CONFERENCE

Pt 1: Noise (and Introductory Matter)

1. A.W. Pryce, "Keynote address: Underwater acoustics — modelling".
2. P. Wille, "Noise sources in the ocean, Pt I".
3. M. Daintith, "Noise sources in the ocean, Pt II".
4. H. Cox, "Acoustic noise models".

Pt 2: Bubbles

5. B. Williams & L. Foster, "Gas bubbles in the sea: A review and model proposals".
6. H. Medwin, "Acoustical probing for microbubbles at sea".

Pt 3: Sea surface

7. C.R. Ward, "A spectral ocean wave model".
8. H. Schwarze, "A theoretical model for doppler spread of backscattered sound from a composite-roughness sea surface".
9. O.I. Diachok, "Effects of sea-ice ridges on sound propagation in the Arctic Ocean".
10. J. Siebert, "Low-frequency acoustic measurements in a shallow-water area with a rough sea surface".
11. P.A. Crowther, "Surface wave spectra".
12. H. Trinkaus, "Scattering and reflection of sound from the sea surface".

Pt 4: Sea bottom

13. F.M. Phelan, B. Williams & F.H. Fisher, "Highlights of bottom topography inferred from received depression and bearing angles".
14. S.R. Santaniello & F.R. Dinapoli, "Ocean-bottom reflectivity (a point of view)".
15. W.A. Kuperman & F. Ingenito, "Relative contribution of surface roughness and bottom attenuation to propagation loss in shallow water".
16. R.E. Christiensen & W.H. Geddes, "Refraction of sound in the sea floor".
17. J.A. Desanto, "Scattering from a random interface".
18. E.L. Hamilton, "Acoustic properties of the sea floor".
19. H. Bucker & H. Morris, "Reflection of sound from a layered ocean bottom".
20. B. Hurdle, K.D. Flowers & J.A. Desanto, "Acoustic scattering from rough surfaces".

Pt 5: Macro-scale phenomena

21. W. Munk, "Acoustic scintillations of acoustic waves".
22. S. Flatté, "Intensity and phase fluctuations in low-frequency acoustic transmission through internal waves".
23. T.H. Bell, Jr., J.M. Bergin, J.P. Dougan, Z.C.B. Hamilton, W.D. Morris, B.S. Okawa, E.E. Rudd & J. Witting, "Two-dimensional internal-wave spectra".
24. I.M. Blatstein, "Ocean-basin reverberation from large underwater explosions, Pt I: Source-level and propagation-loss modelling".
25. J.A. Goertner, "Ocean-basin reverberation from large underwater explosions, Pt II: Computer model for reverberation".
26. J.D. Shaffer, R.M. Fitzgerald & A.N. Guthrie, "Some effects of large-scale oceanography on acoustic propagation".
27. H.H. Essen, "Influence of internal waves on sound propagation in the SOFAR channel".
28. O.M. Johannessen, "A review of oceanic fronts".
29. R. Mellen & D.G. Browning, "Some acoustic effects of internal macrostructure".

Pt 6: Micro-scale phenomena

30. D.R. Del Balzo & W.B. Moseley, "Random temperature structure as a factor in long-range propagation".
31. J.J. McCoy, "Beam spreading and loss of spatial coherence in an inhomogeneous and fluctuating ocean".
32. R. Tait, "Internal oceanographic microstructure phenomena".
33. D. Mintzer, "Acoustic effects of internal microstructure".

Pt 7: Field calculations

34. S.N. Wolf, "Measurements of normal-mode amplitude functions in a nearly-stratified medium".
35. R.D. Graves, A. Nagl, H. Uberall, A.J. Haug & G.L. Zarur, "Range-dependent normal modes in underwater sound propagation".
36. J.A. Desanto, "Inverse wave propagation in an inhomogeneous waveguide".
37. A. Gille & D. Odero, "A solution of the wave sound equation in shallow water for real-speed profiles and solid bottom under-sediment".
38. D.J. Ramsdale, "A wave-theoretic method for estimating the effects of internal tides on acoustic wave transmission".
39. J.G. Schothorst, "Effect of ship motion on sonar detection performance".
40. C.W. Spofford & H. Garon, "Deterministic methods of sound-field computation".
41. R. Goodman, "Stochastic methods of sound-field computation".

Pt 8: Sonar models

42. B.B. Adams & G.R. Giellis, "A technique of comparative analysis of underwater-sound-transmission loss curves".
43. J.A. Desanto, "Connection between the solution of the Helmholtz and parabolic equations for sound propagation".
44. F. Dinapoli, "Computer models for underwater-sound propagation".
45. D. Wood, "Assessment techniques for computer models of sound propagation".

TABLE OF CONTENTS

Pt 6: Micro-scale Phenomena

(Total number of printed pages in this document: 72)

RANDOM TEMPERATURE STRUCTURE AS A FACTOR IN LONG RANGE PROPAGATION

by

D.R. DEL BALZO and W.B. MOSELEY
Naval Research Laboratory
Washington, D.C.
U.S.A.

ABSTRACT

A statistical description of horizontal thermal microstructure in anosotropic turbulence is developed for application with an existing acoustic propagation theory. The model predicts a temperature power density spectrum which decays as -5/3 and -3 in the convective and buoyancy ranges, respectively. The relative power in the two ranges is a function of depth and depends on the total rate of energy dissipation, the total rate of dissipation of temperature variance, and the Brunt-Väisälä frequency. Companion experimental data at two widely separated stations of the North Atlantic verify the theoretical predictions.

INTRODUCTION

This paper presents models and measurements both for the horizontal oceanic random temperature field and for the horizontal transverse correlation of the acoustic energy which has propagated through a random environmental field. First the environmental field model is discussed and measurements supporting the model are presented. Then a theoretical solution for the acoustic correlation function which incorporates the environmental field properties is compared with acoustic data.

A considerable amount of effort by a number of researchers has been devoted to the description of the random horizontal temperature structure of the oceans. This effort has produced a variety of single term power law representations of this structure, particularly in the wavenumber range between internal waves and dissipation. This intermediate range is treated both theoretically and experimentally in this paper. It is shown that two physical processes, buoyancy and convection, have a depth dependent effect on certain scale sizes of the temperature microstructure spectrum which can result in a number of single term power law representations. The form of the temperature power spectral density curve, which is developed and observed within the anisotropic buoyancy-convective wavenumber range, is strongly influenced by the Väisälä frequency, N.

ENVIRONMENTAL THEORY

The first step in the theoretical treatment,[Moseley and DelBalzo, 1974], of horizontal spatial temperature fluctuations in an anisotropic ocean throughout the buoyancy-convective range involves a modification of the standard assumptions (Corrsin, 1951) applicable in an isotropic medium. The modified assumptions are listed below.

1. Temperature is not a simple passive additive. Although the temperature fluctuations are still so small as to have no appreciable effect on the velocity field, the mean temperature gradient, through its effect on density, does directly influence the velocity structure.

2. The mean density gradient is statically stable.

3. The statistical properties of both temperature and velocity in the spectral range of interest are homogeneous and isotropic only in horizontal planes and are stationary.

4. With the exception of scaling and dimensionalizing factors, the statistical properties of the temperature fluctuations are

determined solely by (a) D_θ, the temperature variance flow rate through the buoyancy-convective range; (b) ε_o, the viscous energy dissipation rate; and (c) the energy spectrum in the buoyancy-inertial range of velocity fluctuations (Lumley, 1964).

A dimensional analysis, based on the above assumptions, yields

$$T_{BC}(k) = A_1 k^{-5/3} + A_2 k^{-3} \qquad (1)$$

where $A_1 = BD_\theta \varepsilon_o^{-1/3}$ and $A_2 = BCD_\theta \varepsilon_o^{-1} N^2$ with B and C being dimensionless constants of order one. The first term results from convective turbulence; the second term occurs due to the buoyancy influence on the turbulence. The coefficient of the second term has an explicit dependence on the Brunt-Väisälä frequency.

There are a number of predictions that can be made on the basis of this simple formulation. We shall just treat a couple. First, if the wavenumber interval under analysis is the fixed interval $[k_L, k_u]$ and a single-term power law analysis is applied, then the value of the resulting exponent would be expected to vary in depth in a manner similar to the Väisälä frequency. This occurs because the relative dominance of the second term increases as the Väisälä frequency increases and so the single-term power law approximation begins to approach -3. Conversely, as the Vaisala frequency decreases, the influence of the second term decreases and the single-term approximation provides a power law close to -5/3. This effect is depicted in figure 1 where the transition wavenumbers k_b and k'_b (above which inertial turbulence is the dominant influence) correspond to large and small values of N, respectively.

A second theoretical prediction would be that if one plotted the power law resulting from a single-term analysis versus the square of the local Väisälä frequency, one would expect the power law to be asymptotic towards 3 as the Väisälä frequency increases.

In summary, this development shows a two-term power law for temperature fluctuations in the buoyancy-convective range of wavenumbers. The spectral decay associated with buoyancy is shown to be proportional to k^{-3}, and the decay associated with convection is proportional to $k^{-5/3}$.

ENVIRONMENTAL MEASUREMENTS

A series of environmental measurements (temperature, sound speed, pressure and rate of advance) were taken along 54 straight horizontal tows near Bermuda over a wide range of depths, speeds and distances. Spatial power density spectra of temperature fluctuations after

removal of a mean and linear trend were computed and corrected for depth variability for each of the runs.

In all of the treatments that follow, logarithms were taken to equalize the variance of the power density estimates before the least square analysis procedure was applied.

Figure 2 indicates the results of single-term power law analyses over a fixed wavenumber interval versus depth. The symbols denote the power law values obtained and the vertical bars indicate the 90% confidence limits. As predicted, the single-term power law varies between -5/3 and -3. The dependence on depth was strongly suggestive of the Väisälä frequency profile for the area. In figure 3 the exponent resulting from the single-term analysis is graphed as a function of the temperature gradient (which is proportional to the square of the Väisälä frequency) and the predicted asymptotic approach toward -3 for large N should be noted.

Figure 4 illustrates schematically the components of a procedure to check the details of the theory via a separated two-term analysis. If the initial wavenumber interval under analysis is constrained to sufficiently large wavenumbers, the influence of the -3 power law term becomes negligible. In this restricted wavenumber interval, a single-term power law analysis provides experimental estimates of the coefficient and exponent for the -5/3 term. Next an analysis is performed over the entire wavenumber interval throughout which the contributions (as determined from the experimental coefficient and exponent) of the -5/3 term are treated as noise and removed from the total temperature power spectrum. A single-term power law analysis is performed on the residual and this gives experimental estimates of the coefficient and exponent for the -3 term.

Our measurements extended to the large wavenumbers required by this procedure in 19 of the 54 tow runs. The average value of the exponent in the constrained high wavenumber interval was -1.68, extremely close to the theoretical value of -5/3. Having removed the contributions of this term, the power law analysis on the residual gave an average value for the exponent of -2.94, again close to the theoretical value of -3. In figure 5, for each run, the experimental estimate for the exponent of the term dominant in the buoyancy interval is plotted versus the experimental estimate for the exponent of the term dominant in the convective interval. μ indicates the mean power law in the buoyancy interval. The 90 % confidence limits on this mean include the value -3. Thus, we conclude that the mean is not significantly different from -3, and that the experimental data support the environmental theory in the buoyancy-convective wavenumber range.

The environmental model which is to be incorporated in a propagation theory should include the range of wavenumbers dominated by internal waves. The power spectrum for this lower wavenumber interval can be obtained from Garrett and Munk (1975).

ACOUSTIC MODELING AND MEASUREMENT

Equipped with a model of random horizontal temperature fluctuations, we now briefly assess an influence of these fluctuations on acoustic propagation. In particular the two-point acoustic correlation function at the receiver is investigated because it is a low-order statistic directly relevant to system performance. Γ, the acoustic correlation function is defined as

$$\Gamma(\underline{x}_1, \underline{x}_2) = \{P(\underline{x}_1)\, P^*(\underline{x}_2)\}$$

the ensemble average of the product of the acoustic pressure at one point in the field and the complex conjugate of the acoustic pressure at a second point in the domain.

Starting from the reduced wave equation satisfied by the acoustic pressure at each of two points in the field, one can derive via the operator-smoothing method an integro-differential equation governing the propagation of the acoustic correlation function:

$$\begin{aligned}
&[\nabla_1^2 + k^2(\underline{x}_1)]\,[\nabla_2^2 + k^2(\underline{x}_2)]\,\Gamma(\underline{x}_1, \underline{x}_2) \\
&- [\nabla_1^2 + k^2(\underline{x}_1)]\left[k^2(\underline{x}_2)\int G(\underline{x}_2, \underline{\rho})\, k^2(\underline{\rho})\, R_\epsilon(\underline{x}_2, \underline{\rho})\,\Gamma(\underline{x}_1, \underline{\rho})\, d\underline{\rho}\right] \\
&- [\nabla_2^2 + k^2(\underline{x}_2)]\left[k^2(\underline{x}_1)\int G(\underline{x}_1, \underline{\eta})\, k^2(\underline{\eta})\, R_\epsilon(\underline{x}_1, \underline{\eta})\,\Gamma(\underline{\eta}, \underline{x}_2)\, d\underline{\eta}\right] \\
&+ k^2(\underline{x}_1)\, k^2(\underline{x}_2)\, R_\epsilon(\underline{x}_1, \underline{x}_2)\,\Gamma(\underline{x}_1, \underline{x}_2) = 0
\end{aligned}$$

In this equation, G is the Green's function for the reduced deterministic wave equation, k is the deterministic acoustic wavenumber, and R_ϵ is the two-point correlation function for the random environmental field. A weak environmental field assumption has been made so truncation of the infinite series of integral operators can be accomplished at the order requiring only the two-point statistic of the environmental field.

Two approaches toward solving for Γ are currently being implemented. In the first approach a parabolic equation approximation is introduced and then a computer based numerical solution is constructed. This technique allows inclusion of actually observed oceanic sound speed profiles as well as the random environmental field.

The second approach involves additional assumptions which provide a strictly differential equation formulation and subsequently allow a closed form solution. It is a solution resulting from the second approach that will be compared with acoustic measurements in this paper. The closed form solution derived by McCoy and Beran (1975) and shown below retains the basic anisotropic nature of the two-point environmental statistic together with the approximate form of the power spectrum of random temperature fluctuations in the horizontal plane.

$$\Gamma(L, F, y) = I \exp\left[-E F^{5/2} L y^{3/2}\right]$$

This result states that the acoustic correlation function along a horizontal line transverse to the direction of propagation is an exponential function whose argument is proportional to: E, an environmental factor; the frequency F to the 5/2 power; L, the range; and the transverse horizontal separation distance, Y to the 3/2 power. I is the intensity at a point receiver with the same range and depth. The factors of the environmental parameter are given in detail in the next equation.

$$E = 1.76 \left[\frac{1}{C_o}\frac{\partial C_o}{\partial T}\right]^2 A_T \, l_{ym} \left[2\pi/C_o\right]^{5/2}$$

Here C_o is the average value of the sound speed, T is temperature, A_T is the strength of the random horizontal temperature variations, and l_{ym} is a length scale associated with the vertical correlation function of the temperature fluctuations. A_T is determined in the following manner: the average value of the Väisälä frequency is determined along the propagation path; then an extrapolation of measured single term coefficient versus Väisälä frequency gives the value utilized.

The comparison of this theoretical solution with acoustic data taken in the same locale as the random temperature data is given in figure 6. Here for a fixed range and fixed frequency the dependence of the correlation function versus increased receiver separation on a horizontal line transverse to the propagation direction is shown. The transverse separation and the range are scaled in units of the acoustic wavelength. The correlation function is scaled by the intensity at a point receiver. The crosses are the experimental values for the average of the cosine of the phase fluctuations which account for the vast majority of the change in the correlation function for a single transmission path as was the experimental case. The solid curve represents the theoretical predictions.

CONCLUSIONS

The assumptions, postulates, and dimensional analysis lead to the

two term formulation

$$T_{BC}(k) = B D_\theta \epsilon_o^{-1/3} k^{-5/3} + BC D_\theta \epsilon_o^{-1} N^2 k^{-3}$$

for the horizontal spatial power density spectrum of random oceanic temperature fluctuations in a wavenumber range called the buoyancy-convective range.

Analysis of experimental data obtained during 54 horizontal tows with depths ranging from 100 to 1450 m supports a number of theoretical predictions. Both the -5/3 and -3 predicted power laws were observed; the mean values were -1.68 and -2.94, respectively.

Upon fitting a single-exponent power law formulation over the entire observation range, the expected power law variation between -5/3 and -3 was seen to occur along with the anticipated asymptotic (to -3) nature of the exponent for increasing magnitude of the Väisälä frequency.

The theoretical predictions together with the experimental evidence in this report provide an explanation for the disparity in experimental results in the field of random temperature microstructure. This environmental theory fills the gap between the wavenumber ranges where internal waves and isotropic turbulence dominate the horizontal spatial random temperature spectrum. The environmental model utilized in the propagation theory formulation should contain the wavenumber ranges dominated by internal waves, buoyancy, and convective turbulence depending upon the acoustic frequency of interest.

The comparison of measured acoustic data and the Beran-McCoy solution for the acoustic correlation function indicates that the theoretical formulation does qualitatively describe the transverse acoustic correlation dependence on receiver separation. The inherent anisotropy and vertical inhomogeneity of the random environmental statistics and the form of the power spectrum for horizontal temperature fluctuations should be included in future theoretical formulations. The quantitative agreement between theory and acoustic measurements indicates that scattering caused by the random temperature field can account for the observed degradation in acoustic correlation for single path transmission.

REFERENCES

1. Beran, M.J. and J.J. McCoy, 1974: Propagation of radiation from a finite beam or source through an anisotropic random medium. *JASA*, 56, 1667-1672.

2. Corrsin, S., 1951: On the spectrum of isotropic temperature fluctuations in an isotropic turbulence. *J. Applied Phys.*, 22, 469-473.

3. Garrett, C. and W. Munk, 1975: Space-time scales of internal waves: A progress report. *J. Geophys. Res.*, 80, 291-297.

4. Lumley, J.L., 1964: The spectrum of nearly inertial turbulence in a stably stratified fluid. *J. Atmos. Sci.*, 21, 99-102.

5. Moseley, W.B. and D.R. DelBalzo, 1974: Oceanic Horizontal random temperature structure. U.S. Naval Research Laboratory Report 7673, Washington, D.C.

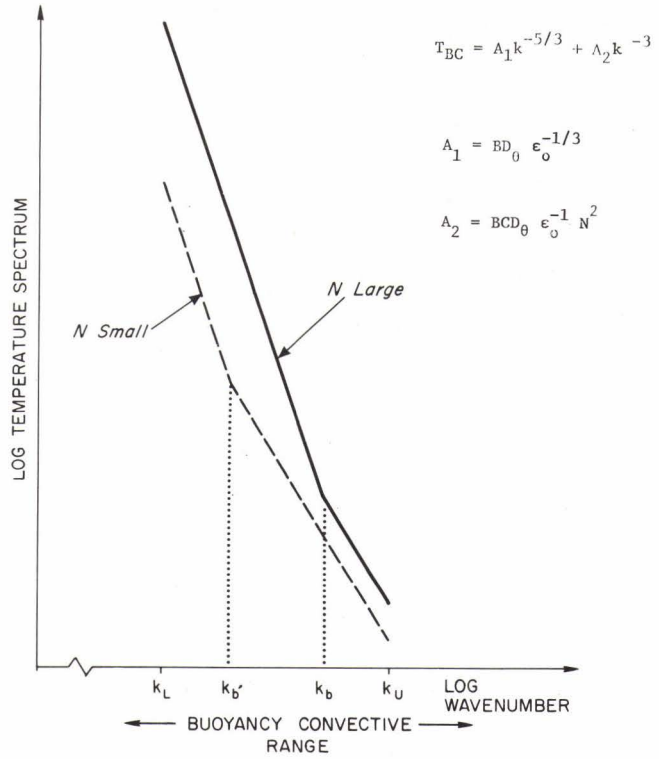

FIG. 1
TEMPERATURE POWER DENSITY SPECTRUM IN BUOYANCY – CONVECTIVE RANGE SHOWING EFFECT OF VAISALA FREQUENCY

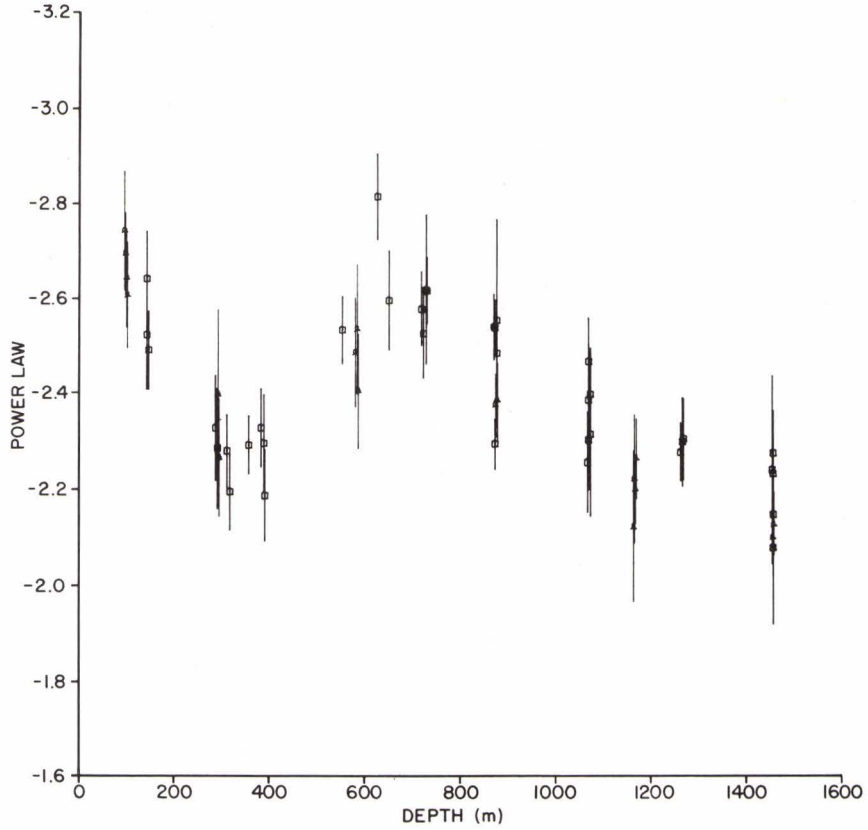

FIG. 2 POWER LAW VS. DEPTH WITH 90% CONFIDENCE LIMITS

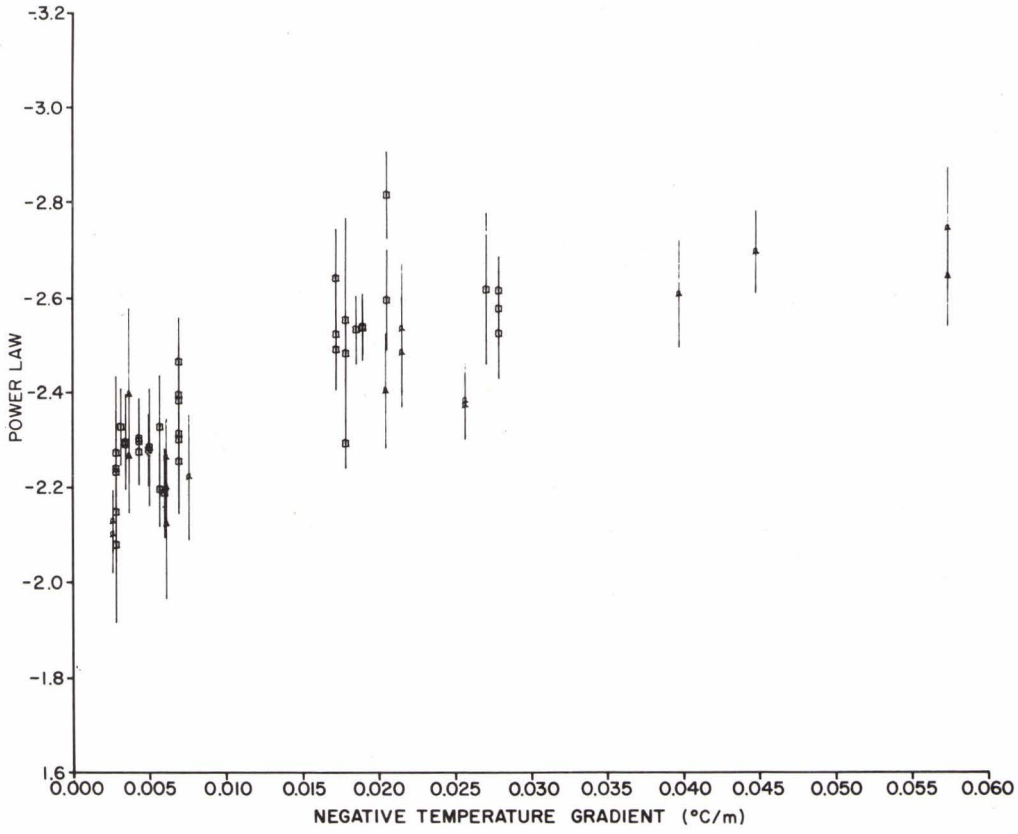

FIG. 3 POWER LAW VS. NEGATIVE TEMPERATURE GRADIENT WITH 90 % CONFIDENCE LIMITS

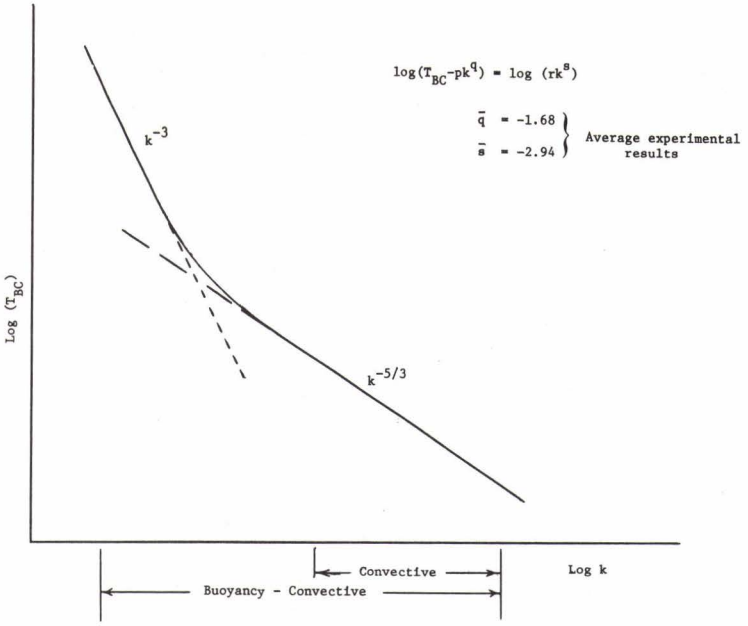

FIG. 4
ANALYZE IN CONVECTIVE RANGE TO OBTAIN ESTIMATES OF p AND q. THEN ANALYZE IN BUOYANCY-CONVECTIVE RANGE WITH ABOVE FORMULA TO OBTAIN ESTIMATES OF r AND s

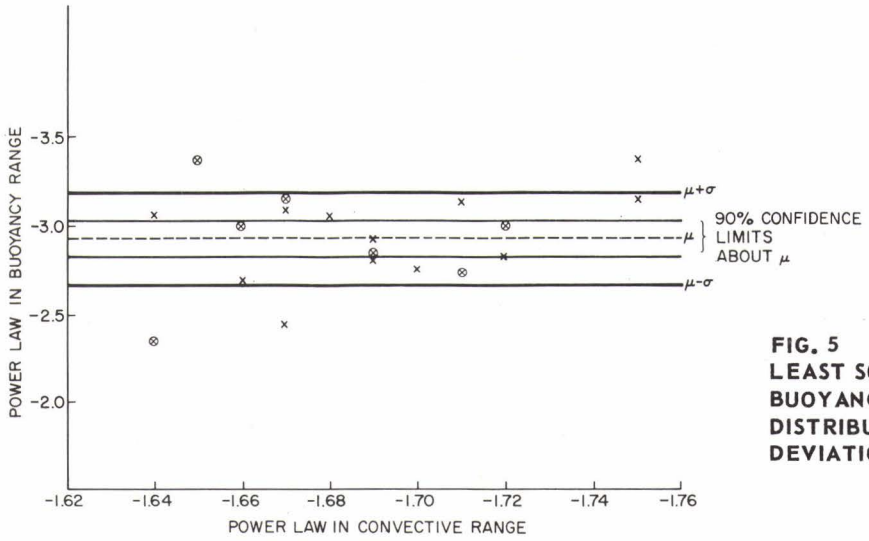

FIG. 5
LEAST SQUARES ANALYSIS ON POWER LAWS IN BUOYANCY AND CONVECTIVE RANGES WITH DISTRIBUTION MEAN, μ, AND ONE STANDARD DEVIATION σ

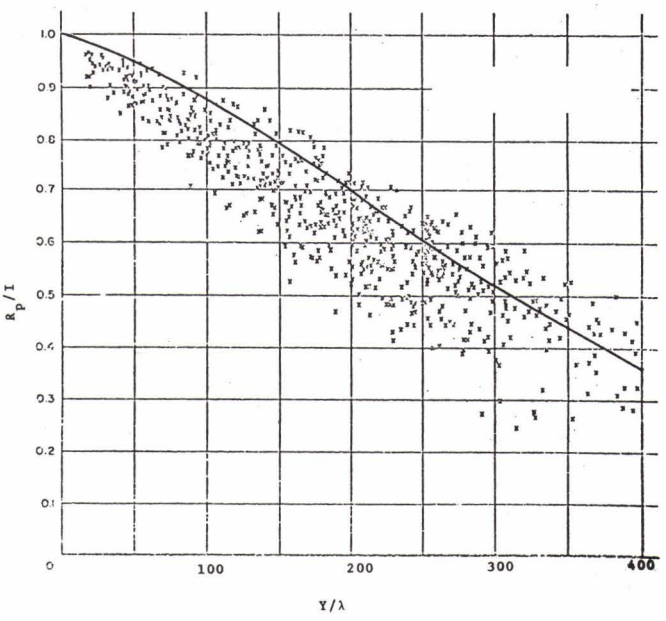

FIG. 6
VARIATION OF ACOUSTIC CORRELATION FUNCTION VERSUS TRANSVERSE SEPARATION BETWEEN RECEIVING ELEMENTS. MEASUREMENTS GIVEN BY x; THE SMOOTH CURVE IS PREDICTED BY THEORY

$$L/\lambda = 0.46 \times 10^5$$

BEAM SPREADING AND LOSS OF SPATIAL COHERENCE IN AN INHOMOGENEOUS AND FLUCTUATING OCEAN

by

JOHN J. McCOY
Naval Research Laboratory, Washington, D.C.

and

Catholic University, Washington, D.C.
U.S.A.

ABSTRACT

A theory has been developed that enables estimates to be made of beam bending, beam spreading and loss of spatial coherence. In this paper we concentrate on the loss of spatial coherence due to scattering. Using a minus two power law as representative of horizontal tow data the solution predicts that the law of coherence of a signal received by a horizontally positioned line array behaves as $I \exp(-Ek^{5/2}ZS^{3/2})$. Here I is the signal intensity, E is an environmental parameter, k is the signal wave number, Z is the range and S is the separation distance between receiver hydrophones.

INTRODUCTION

A propagation model for long-range, low-frequency ocean acoustic experiments should ultimately incorporate the effects of diffraction, refraction and both volume and boundary scatter. In this paper we discuss a model that includes the first three of these factors. The large loss of energy for the portion of an acoustic signal that interacts with the ocean bottom would lead one to suspect that the effects of bottom scatter would be suppressed in a long-range experiment.* Surface scatter effects, however, could be significant and need to be incorporated in an extended model. In applying our model we shall assume that we can isolate, and then suppress, the portion of the acoustic signal that interacts with the surface.

The volume scatter effects incorporated in the model arise due to fluctuations in the sound speed, which are caused by mixing of an inhomogeneous temperature field by dynamic ocean processes; e.g., by internal waves or by ocean turbulence.

The sound field measure in which the model is formulated is the mutual coherence function, which is defined for cw signals according to

$$\{\hat{\Gamma}(\underset{\sim}{x}_1, \underset{\sim}{x}_2, \nu)\} \equiv \{\hat{p}(\underset{\sim}{x}_1, \nu)\hat{p}^*(\underset{\sim}{x}_2, \nu)\} \tag{1}$$

where $\hat{p}(\underset{\sim}{x}, \nu)$ denotes the complex acoustic pressure field; ν, the signal frequency; an asterick, complex conjugation; and the braces, an averaging. The information of interest in the mutual coherence function can be summarized as follows:

i) The collapsed coherence function in which the two points are coincident gives the averaged intensity field, which enables our estimating transmission loss.

ii) The averaged power output of the linear sum of outputs of an (phased) array of hydrophones is given by the coherence function. Thus, it enables the estimation of array signal gain.

iii) The directional decomposition of the energy flux received by an array is directly given by a spatial transform of the coherence function. Thus, it enables an estimation of the loss of resolution due to volume scattering.

Introducing z to denote the range coordinate, the propagation model is expressed in terms of the coherence function measured at two points in the same range plane; i.e.,

---

* This need not be true if the receiving array is bottom-mounted.

$$\{\hat{\Gamma}(\underset{\sim}{x}_{\perp 1}, \underset{\sim}{x}_{\perp 2}, z)\} = \{\hat{p}(\underset{\sim}{x}_{\perp 1}, z)\,\hat{p}^{*}(\underset{\sim}{x}_{\perp 2}, z)\}\,, \tag{2}$$

where $\underset{\sim}{x}_{\perp 1}, \underset{\sim}{x}_{\perp 2}$ denote transverse coordinates. (We henceforth suppress explicit dependence on $\bar{\nu}$ in our notation). The form of the model is, then, written

Rate of Change of $\{\hat{\Gamma}\}$ with Range =

Diffraction Term
\+ Refraction Term
\+ Scattering Terms

Specifically, the mathematical model is given by the partial differential equation

$$\begin{aligned}\frac{\partial}{\partial z}\{\hat{\Gamma}\} = {} & \frac{i}{\langle \bar{k}(z)\rangle}\left(\frac{\partial^2}{\partial p_x \partial s_x} + \frac{\partial^2}{\partial p_y \partial s_y}\right)\{\hat{\Gamma}\} \\ & + i\left[\bar{k}(p_y + s_y/2) - \bar{k}(p_y - s_y/2; z)\right]\{\hat{\Gamma}\} \\ & + \bar{\sigma}_2(\underset{\sim}{s}; p_y; z)\{\hat{\Gamma}(s_x, s_y = 0, \underset{\sim}{p}, z)\} - \bar{\sigma}_2(0; p_y; z)\{\hat{\Gamma}\}\end{aligned} \tag{3}$$

In writing Eq. (3), we have introduced the average and difference transverse coordinates; i.e.,

$$\begin{aligned}\underset{\sim}{p} &= \tfrac{1}{2}(\underset{\sim}{x}_{\perp 1} + \underset{\sim}{x}_{\perp 2}) \\ \underset{\sim}{s} &= \underset{\sim}{x}_{\perp 1} - \underset{\sim}{x}_{\perp 2}\end{aligned} \tag{4}$$

Further, $\bar{k}(y, z)$ denotes the (ensemble) averaged signal wavenumber; i.e., $2\pi\bar{\nu}/\{c\}$; which can vary with range and depth. Also, $\langle \bar{k}(z)\rangle$ denotes the average of $\bar{k}$ taken over the depth. The fluctuations in the sound speed are described by $\bar{\sigma}_2(\underset{\sim}{s}, p_y, z)$, which is given in terms of the correlation function defined on the fluctuating wavenumber by

$$\bar{\sigma}_2(\underset{\sim}{s}, p_y, z) = \left(\frac{2}{\pi}\right)^{1/2}\frac{\bar{k}^3}{4}\int_0^{\infty}\frac{\cos\left(\frac{\bar{k}s_y^2}{2s_z} - \frac{\pi}{4}\right)}{(\bar{k}s_z)^{1/2}}$$

$$\left(\int_{-\infty}^{\infty}\sigma(s_x, s_y', s_z; p_y, z)\,ds_y'\right)ds_z \tag{5}$$

The statistics of the sound speed fluctuations can also be range and depth dependent.

The assumptions made in developing Eq. (3) and the concomitant restrictions on the validity of the model are complex. For details, the reader is referred to a series of papers and reports [1-5]. Briefly, the model requires the validity of the parabolic approximation. (In [4], we show that the equation, without the scattering terms, follows directly from the parabolic equation on the plane wave amplitude field). Thus, the model is restricted to experiments in which the angular distribution of energy flux is limited to "narrow" angles relative to the range direction. Clearly, then, the model requires the scattering to be a narrow-angled scattering. This is shown [1] to be the case for ocean acoustic experiments so long as the acoustic wavelength is short relative to all significant correlation lengths for the sound speed fluctuations measured in a horizontal plane. Further, the model requires that the effects of scattering, diffraction and defraction are all uncoupled over limited ranges. Over extended ranges, the effects are of course coupled. In addition, the model requires that the amount of scattering over limited ranges be small. This is assured by virtue of the weakness of the sound speed fluctuations. Finally, the specific form of the scattering terms is intimately related to the details of the angular distribution of the locally scattered energy. In the ocean acoustic model, which we term an anisotropic model, the sound speed fluctuations are taken such that correlation lengths measured in a horizontal plane are orders of magnitude larger than those measured in the depth direction. The frequency of the acoustic signal is taken to be such that the acoustic wavelenth is of the same order as or larger than the significant correlation lengths measured in the depth direction. The wavelength, as mentioned previously, is assumed to be small relative to horizontal correlation lengths. For much higher frequencies, the signal wavelength will become small relative to correlation lengths measured in the depth direction as well as those in the horizontal plane. In this case, the form of the scattering terms changes and the model becomes that which has been extensively studied in the optics literature [6,7]. This latter model, we refer to as an isotropic model. It is noteworthy that the solutions of the two models are qualitatively different in the multiple scatter region.

In the remainder of this paper we shall briefly outline some special cases in which analytic solutions to the model have been obtained. In particular we discuss three situations.

(1) Homogeneous statistics; absence of a sound speed profile; plane wave incidence: In this case the model is used to determine the spatial correlation for distances separated along a horizontal line. Detailed calculations are carried out for sound speed fluctuations which, when sampled in a horizontal plane, obey a minus two power spectrum.

(2) Homogeneous statistics; a range independent sound speed profile; point and finite coherent sources: In this case the model is used to determine the averaged (taken over the depth) spatial correlation for distances separated along a horizontal line. Thus, the effect of diffraction on the above results is seen.

(3) We briefly consider a solution algorithm based on the model with the scattering term neglected. The algorithm indicates the possibility of predicting beam spreading by appending side calculations to a ray trace program. It should also prove useful for predicting the propagation of signals emanating from partially coherent, or noisy, sources.

Plane Wave Source in a Statistically Homogeneous Fluctuating Ocean

For the case of plane wave incidence and a statistically homogeneous ocean, the diffraction and refraction terms vanish. Equation (3) thus reduces to an ordinary differential equation in the range coordinate, in which the separation coordinates (S_x, S_y) are parameters. The solution is readily obtained and is written

$$\{\hat{\Gamma}(s_x, s_y, z)\} = \hat{I}\left[\frac{\bar{\sigma}_t(s_x, s_y)}{\bar{\sigma}_t(s_x, 0)} \exp\left(-\left[\bar{\sigma}_t(0,0) - \bar{\sigma}_t(s_x, 0)\right]z\right)\right.$$

$$\left. + \left(1 - \frac{\bar{\sigma}_t(s_x, s_y)}{\bar{\sigma}_t(s_x, 0)}\right) \exp\left[-\bar{\sigma}_t(0,0)z\right]\right) \qquad (6)$$

where $\hat{I}$ denotes the intensity of the incident plane wave. For studying the horizontal resolution of a line array positioned orthogonal to the range corrdinate we make use of $\{\hat{\Gamma}(s_x, 0, z)\}$ which is given by

$$\{\hat{\Gamma}(s_x, 0, z)\} = \hat{I} \exp\left(-\left[\bar{\sigma}_t(0,0) - \bar{\sigma}_t(s_x, 0)\right]z\right) \qquad (7)$$

As indicated in the Introduction, the environment is described by the term. In order to obtain a propagation model that requires as input, a few easily measured environmental paramaters we must make a number of assumptions pertaining to the environment.

Included among these are

$$i) \int_{-\infty}^{\infty} \sigma(s_x, s_y', s_z)\, ds_y' = \ell_{yM}\, \sigma(s_x, 0, s_z)$$

$$ii) \quad \sigma(s_x, 0, s_z) = \sigma_M\left(\sqrt{s_x^2 + s_z^2}\right) \tag{8}$$

The first of these assumption leads to a propagation model in which the vertical structure of the fluctuations field is described by a single length scale, ℓ_{yM}. The second assumption is that the horizontal structure is isotropic. Taken together, the environment description required is given by horizontal tow data plus a measure of the length scale for the vertical structure.

The horizontal tow data is more usually presented in terms of the spatial power spectrum, which is given by the Fourier transform of $\sigma_M(\sqrt{s_x^2 + s_z^2})$. We denote this spectrum by $\Phi_1(p)$, where p, here, denotes the transform variable. Our final assumption is to assume that $\Phi_1(p)$ obeys a minus two power law over that portion of the spectrum that contributes significantly to the scattering. It is important to realize that a justification for choosing a functional form for $\Phi_1(p)$ requires some knowledge of which length scales defined by the fluctuating sound speed field are important. This, in turn, depends on the acoustic experiment that is of interest. That is, the justification can only be argued, a posteori. For the low frequency experiments for which the model was developed, we have demonstrated [3] that the important length scales are moderately large (500-5000 m.), for which the minus two law has attained a degree of acceptance.

With the above assumptions of the environment, we can reduce the exponent in Eq. (7) to a simple algebraic form,

$$\{\hat{I}(s_x, 0, z)\} = \hat{I} \exp\left[-E(\bar{k}s_x)^{3/2}(\bar{k}z)\right] \tag{9}$$

The environment is described for Eq. (9) by a single nondimensional parameter, E, which is given in terms of measured data according to

$$E = 1.76 \times 10^{-5} A_T^2 \ell_{yM} \tag{10}$$

where A_T^2 is obtained by fitting a minus two law to horizontal tow data of temperature fluctuations. The units of A_T^2 is $(^oC)^2$/length.

Equation (9) represents a particularly simple expression for estimating the loss of spatial coherence due to scattering from large scale ocean temperature fluctuations. A comparison has been made between predictions made by it and archival experimental data and the results are very encouraging. The classification of some of the archival data presents my showing these results at this session. The comparison will be available, however, in an article to be submitted to JUA [8].

Effect of Finite Source Size and a Depth Dependent Sound Speed Profile

We consider next a calculation in which the sound speed is taken to vary with depth and the source is taken to have a finite size. The fluctuations in sound speed are still taken to be statistically homogeneous. The quantity to be calculated is

$$\langle \{\hat{\Gamma}(p_x, s_x, z)\} \rangle = \frac{1}{H} \int_0^H \{\hat{\Gamma}(p_x, s_x, p_y, 0, z)\}\, dp_y \tag{11}$$

where H is envisioned to span the sound channel. The quantity $\langle\{\hat{\Gamma}\}\rangle$ is interpreted to be an averaged coherence function for two points located on the same horizontal line that is orthogonal to the principal propagation direction. Thus, it provides a measure of an averaged loss of horizontal resolution.

For $\bar{\sigma}_z$ independent of P_y, we can average Eq. (3) and obtain the following equation on $\langle\{\hat{\Gamma}\}\rangle$ [3]

$$\frac{\partial \langle\{\hat{\Gamma}\}\rangle}{\partial z} = \frac{i}{\langle \bar{k} \rangle} \frac{\partial^2 \langle\{\hat{\Gamma}\}\rangle}{\partial p_x \partial s_x} + \langle \bar{k}^2 \rangle \left[\bar{\sigma}_z(s_x, 0) - \bar{\sigma}_z(0,0)\right] \langle\{\hat{\Gamma}\}\rangle \tag{12}$$

where $\langle \bar{k} \rangle$ is the spatially averaged, mean wavenumber. Equation (12) shows that there is no effect of a depth dependent sound speed on the averaged (taken over the depth) horizontal resolution. We note that the presence of depth dependent statistics for the sound speed fluctuations cannot be treated so easily.

In [2], we consider solutions of Eq. (12). The "source" for these calculations is located in the z=0 plane, which is taken to be a constant phase plane. The intensity distribution across the source is taken to be Gaussian. We calculated $\langle \{\hat{\Gamma}(0, s_x, z)\} \rangle$, which provides an estimate of the loss of signal coherence along the beam center. The

results differ in the numerical factor in the definition of E. For a point source (a Gaussian intensity distribution in which the horizontal beam width is zero), the numerical factor is 0.7×10^{-5}; for a finite source the factor is smaller still. Thus, the coherence of a signal emanating from a point source decays more slowly than that from a plane wave source; the coherence of a signal emanating from a finite source decays more slowly than those from either of the two limits.

$\langle \{ \hat{I}(P_x, 0, z) \} \rangle$

on the averaged intensity measured across the sound channel. This enables estimates of the dependence of beam spread on diffraction and on scattering. In the limits in which one or the other of these mechanisms is predominant, simple analytic results were obtained. Thus, for conditions in which diffraction effects are predominant, the beam width increases with range as $(a^2 + z^2/k^2\ a^2)\ 1/2$, where "a" is the initial beam width. For conditions in which scattering effects are predominant, the length scale for observing variations in intensity is of the order of $(E^{2/3}\ k\ 2/3\ Z^{5/3})$. For an intermediate case in which scattering and diffraction effects are both important, it is necessary to resort to automatic computation. The interested reader is referred to [2].

Propagation in Nonfluctuating Media

Equation (3) minus the last two terms serves as the basis of an acoustic model for experiments in which volume scatter is not significant. In [4], we show the equation to follow directly from a parabolic equation written on the plane wave amplitude. Any "randomness" of the radiation field for this deterministic medium problem enters via the source. Thus, for example, one might be interested in sound emanating from a partially coherent, or noisy source. Or, one might be interested in sound that has passed through a fluctuating region of an otherwise deterministic medium. Problems of stochastic sources have received a good deal of attention in treating electromagnetic radiation fields. An equation similar to Eq. (3) with no scattering terms could be used to formulate the theory of partial coherence as it is termed in this latter literature.

Further, since a deterministic radiation field can be interpreted as a limiting case of a stochastic radiation field, in which all manifestations of the experiment are identical, Eq. (3) minus the scattering terms could be applied to a purely deterministic problem. With reference to this, however, we note that the dimensions of the space on which Eq. (3) is defined are five in number, whereas the purabolic equation on the plane wave amplitude itself is defined on a three dimensional space. Thus, in general, it would appear to be easier, in treating a deterministic problem, to first solve for the pressure field and then, if desired, calculate the intensity field or the "coherence" field. The value of a model based on Eq. (3) for treating deterministic fields would then rest simply in the unification that it brings to treating a spectrum of problems. As indicated below, however, the value

of a model based on Eq. (3) may, for a class of deterministic problems, be more extensive than this.

Consider Eq. (3), with no scattering terms, and introduce an approximation based on expanding and truncating the $k(P_y \pm S_{y/z}; Z)$ terms appearing therein. A truncation after the quadratic term leads to the following approximate equation,

$$\frac{\partial\{\hat{\Gamma}\}}{\partial z} = \frac{1}{\langle \bar{k}(z)\rangle}\left(\frac{\partial^2}{\partial p_x^2 S_x} + \frac{\partial^2}{\partial p_y^2 S_y}\right)\{\hat{\Gamma}\} + i\frac{d\bar{k}(p_y)}{dp_y} S_y \{\hat{\Gamma}\}. \tag{13}$$

In [4], we discuss in some detail the validity of Eq. (13) for both the stochastic and deterministic source problems. Briefly, for the former the requirement is that spatial extent of the region over which the resulting field is coherent must be small relative to the length scales on which $k(P_y)$ vary. For narrow beamed deterministic signals the validity can be argued on the assumption that the beam width is small on the length scales on which $k(P_y)$ vary. For broad beamed deterministic signals, the validity can still be argued over limited ranges.

To solve Eq. (13), we first introduce a spatial Fourier transform of the separation coordinate. Denoting by S, the transform variable, the equation on $\{\tilde{\Gamma}(p_x, \xi, z)\}$ is then written

$$\frac{\partial\{\tilde{\Gamma}\}}{\partial z} = \frac{1}{\langle \bar{k}(z)\rangle}\left(\xi_x \frac{\partial}{\partial p_x} + \xi_y \frac{\partial}{\partial p_y}\right)\{\tilde{\Gamma}\} + \frac{d\bar{k}(p_y)}{dp_y}\frac{\partial\{\tilde{\Gamma}\}}{\partial \xi_y} \tag{14}$$

This equation is recognized as a first order partial differential equation. Thus, a general solution procedure exists for its inversion, which requires that we first construct its characteristics. Then, an ordinary differential equation (in this case of first order) is written on the change of $\{\hat{P}\}$ with distance measured along the characteristic and is solved. To determine $\{\hat{P}\}$ requires that we transform back to $\underset{\sim}{s}$ space. Excluding the algorithms required by the transformation into and out of $\underset{\sim}{s}$ space, the principal numerical task in carrying out the above procedure is the construction of the characteristics. These, moreover, can be identified with the rays of the geometric theory suggesting the possibility of appending the needed added calculations to an existing ray trace program. In this way, diffraction effects can be incorporated in a geometric theory program by carrying along some side calculations. The effects of scattering apparently cannot be introduced in such a simple manner.

We have considered a number of problems for which Eq. (13) is exact, within the context of the parabolic approximation, and for which we could carry out the above described solution procedure analytically. The solutions obtained exhibit the qualitative behavior expected; e.g., beam bending, beam spreading due to diffraction, beam focusing in a sound channel, a characteristic oscillatory behavior in the intensity field in the neighborhood of caustics, etc. These analytic solutions are being used to test some of our numerical routines that are nominally based on a parabolic approximation.

Acknowledgment

The support of the U.S. Naval Electronics Systems Command through the U.S. Naval Research Laboratory is gratefully acknowledged.

References

1) Beran, M.J. and McCoy, J.J., "Propagation through an Anisotropic Random Medium", J. Math. Phys. 15, 11, 1901 (1974).

2) Beran, M.J. and McCoy, J.J., "Propagation of Radiation from a Finite Beam or Source through an Anisotropic Random Medium", J. Acous. Soc. Am. 56, 6, 1667 (1974).

3) Beran, M.J. and McCoy, J.J. and Adams, B.B., "Effects of a Fluctuating Temperature Field on the Spatial Coherence of Acoustic Signals", NRL Report 7809 (1975).

4. McCoy, J.J. and Beran M.J., "Propagation of Beamed Signals Through Inhomogeneous Media - A Diffraction Theory", submitted for publication.

5) Beran, J.J. and McCoy J.J., "Propagation Through an Anisotropic Random Medium - An Integro-Differential Formulation", submitted for publication.

REVIEW PAPERS

INTERNAL OCEANOGRAPHIC MICROSTRUCTURE PHENOMENA

by

R.I. Tait
SACLANT ASW Research Centre
La Spezia, Italy

ABSTRACT

This paper is concerned with the nature and causes of both fine structure and microstructure in the ocean. Following an account of the acoustic/oceanographic background to subject, the characteristics of fine structure are described in terms of temperature and salinity profiles from the N.E. Atlantic. The three main causal mechanisms, horizontal advection, shear instability and double diffusion are discussed and their relative importance to fine scale phenomena is assessed. Microstructure observations from high resolution free fall instruments are used to illustrate the main features of the true microscale. These data provide evidence for the presence of both shear instability and double diffusive mechanisms. An examination of the relationship between the fine and micro scales leads to the conclusion that within an otherwise "quiet" ocean intensive vertical mixing occurs sporadically in specific areas characterized by the presence of an appreciable fine structure.

INTRODUCTION

It is now well established that the oceans are not smoothly stratified. When we look at the fine-scale structure, i.e. at the scale structure with vertical wave number of $K < 1.0$ cycle/metre which is the range covered by the standard STD, we find numerous inversions in temperature salinity and also mixed layers separated by interfaces where the gradients are relatively sharp. At higher wave numbers, $K > 1.0$ cycle/m, which is defined as the microstructure range, the new generation of instruments currently under development have revealed that this situation continues right down to the diffusive cutoff scales* of the order of a few centimetres. The situation is illustrated in Fig. 1.

In reviewing the field of microstructure, it is particularly appropriate at this meeting to acknowledge the early role played by acousticians. The existence in the ocean of a finer structure than the classical two-layer picture first became apparent during World War II when the scintillation of sound waves observed during sonar experiments was attributed to the presence of small isotropic scatterers. Although evidence of fine thermal stratification was known from BT's, acousticians preferred to study the temperature fluctuations horizontally rather than vertically, in the same direction as the propagation. Extensive work of this nature between say the late 1940's and early 1960's gave rise to an ocean model composed of small random thermal scatterers that were statistically spheroidal. Although this concept of thermal patches of dimension ~1 m was, perhaps still is, acceptable to acousticians it is far from realistic from the oceanographic point of view.

Now what were the oceanographers doing during this period? It so happened that during the time when the acousticians were working with high-resolution equipment, which identified the effects of small-scale features, oceanographers were concerned with large-scale low-frequency oceanic structures and movements as revealed by Nansen bottles. The dialogue between acoustics and oceanography appeared to be at a low ebb**. This was not the fault of the oceanographers: they had no instrumentation available for fine structure profiling in the ocean.

---

* The division as defined above between fine structure and microstructure corresponds approximately to a wave number $K_B = \frac{1}{2\pi}\left(\frac{N^3}{\varepsilon}\right)^{\frac{1}{2}}$ which represents the scale of the largest eddies that can be considered isotropic. The diffusive cut-off scales for velocity and temperature are given respectively by $K_v = \frac{1}{2\pi}\left(\frac{\varepsilon}{\nu^3}\right)^{\frac{1}{4}}$ and $K_T = \frac{1}{2\pi}\left(\frac{\varepsilon}{\nu K_T^2}\right)^{\frac{1}{4}}$.

** Paradoxically, as was pointed out by Bethell 1972 , when oceanographers did become interested in fine structure it seemed as though acousticians began to loose interest, e.g., the 1950-70 Review of Underwater Acoustics by Berman Guthrie 1972 where the section on thermal microstructure contains references dated no later than 1963.

1. FINE-SCALE STRUCTURE

Intensive oceanographic interest in fine structure measured vertically stems from the development of STD systems in USA and Europe in the early 1960's. It is worth remembering that the STD was developed as a modern replacement for the traditional Nansen cast, over which it had obvious advantages, but its full value did not become apparent until it began to be used at sea, when the degree of fine structure observed came as a distinct surprise. Clearly here was a phenomenon of great interest and well worth studying.

At Liverpool University we were fortunate in acquiring in 1965 one of the earlier STD's, the Hytec 9006. In the summer of 1966 my colleagues and I made the first STD observations of the Mediterranean outflow in the NE Atlantic. In spite of hints from the earlier work of Cooper [1967] in this area with closely-spaced water bottles the degree of fine structure found was unexpected.

Figure 2 shows a plot of the original analogue record for a station about 100 miles west of Lisbon. I have three reasons for showing this:

1. It has historical value and the data have not been published.

2. It is typical of the T & S profiles found not only in this area but also wherever we have the intrusion of a discordant water mass of different origin.

3. I can use it to illustrate several points concerning fine structure.

Our main concern is with the section of the record from 300 m to 1500 m corresponding to the depth scale on the right. The horizontal scales span 5°(15° to 10°) and 2‰ (36.5‰ to 34.5‰) for T & S respectively. On the largest structure scale we have the main feature of the high S & T bulge of the Mediterranean water separated above and below from the Atlantic water by two boundary zones where the mean vertical gradients are relatively large and of opposite sign. The main salinity maximum is apparent at the usual depth for this region of 1200 m, but we also have another secondary maximum at about 800 m which is particularly apparent on the T trace (right). The Mediterranean water is thus divided here into two main water types, the upper being warmer and therefore of lower density. This upper water, which has been the subject of a long term investigation at Liverpool University, has also been discussed by Siedler [1968], Madelain [1970], Zenk [1970 & 1975], and Howe and Abdullah [1974]. It is considered to be Mediterranean water that has been subjected to a different mixing history from that of the main stream of Mediterranean outflow.

If we now look at the smaller-scale effects we find apparently random temperature inversions occurring throughout the column, from a few tens of metres in thickness down to the STD cutoff scale

at about 2 m. The presence of thermal structure below this in the true microstructure range is apparent from the S trace, which at the smallest scale reflects conductivity rather than salinity. On the medium scale every T change has an associated S change and the two invariably combine to produce a stable relatively-smooth density profile. This is most easily seen on a T/S diagram. I have labelled various key points on both traces in Fig. 2 and the corresponding T/S plot is given in Fig. 3. The inversion layers tend to run parallel to the isopycnals but show a general downward progression with each successive point, implying that the stratification is statically stable.

Since 1966 the medium-scale structure associated with the Mediterranean outflow has been studied by Tait and Howe [1968, 1971], Pingree [1969, 1971], Zenk [1970, 1975], Katz [1970] and many others over a wide area from Finisterre to Madeira and out as far as the Azores. Going even further afield, Ichye and Sudo [1971] have detected the Mediterranean water in the Caribbean and the Gulf of Mexico.

Figure 4 shows a processed record, again from the Mediterranean outflow area, due to Pingree [1970]. The position is 160 miles SW of Finisterre. The fine structure features are similar and shown also are the calculated profiles for potential density σ_θ and specific volume anomaly δ. The apparent instability in the lower part of the σ_θ profile is due to a compressibility effect. In this region of large negative temperature gradient, $\frac{d\sigma_\theta}{dz}$ does not reflect the true stability of the water column, and one must take the increasing compressibility of the cooler water into account. Pingree shows that under these conditions the stability is better related to the δ gradient but the more conventional approach is now to estimate stability in terms of the Väisälä frequency, N, given by $N^2 = \frac{g}{\rho}\frac{\partial \rho}{\partial z} - \frac{g^2}{c^2}$, where $\frac{\partial \rho}{\partial z}$ is the in-situ density gradient. Results from other similar oceanic areas, i.e. similar in the sense of the presence of different water masses e.g. Gregg and Cox [1972] in the Pacific; Gilmour [1972], in the Mediterranean; Hamon [1967] in the Indian Ocean have given the same general picture regarding the fine structure. Two main general conclusions can be drawn from this work.

1. The ratio between the horizontal and vertical scales for inversions seems to be of the order of 10^3. This general relationship appears to apply over a wide range of scales and also the other types of stratification such as the step structures associated with the thermocline described by Cooper and Stommel [1968].

2. The temperature and salinity changes are highly correlated and density compensating, leading to a stable density profile.

2. CAUSES OF FINE-SCALE STRUCTURE

The above observations, together with the fact that the fluctuations are aligned with constant-density surfaces, suggest that the structures are formed by the lateral interleaving of different water types, i.e. by horizontal advection. It was, I think, Phillips who stated recently that "it is almost certain that not all the fine structure found in the ocean can be ascribed to a single mechanism".

The three most likely mechanisms involved in the medium-scale structure are:

1. Advective processes.
2. Wave-induced shear instability; Billow turbulence.
3. Double diffusion.

All have been extensively discussed in the literature. The most comprehensive quantitative experiments on double diffusion (i.e. diffusion processes related to the different molecular diffusivities of heat and salt), particularly on the phenomenon known as salt fingering, are those of Turner and his associates at Cambridge, e.g. Turner and Stommel [1964], Turner [1967, 1968], Stern and Turner [1969], Shirtcliffe and Turner [1970], Huppert and Turner [1972], Linden [1973].

Many attempts have been made to apply the theoretical results to the ocean, seeing in the oceanographic data a reflection of the phenomena produced in the laboratory. K.N. Federov has been particularly active in this respect: Federov [1970] applied the double-diffusion theory applicable to the heating of a salt gradient from below to Zenk's observations of the Mediterranean water and was criticized for so doing by Huppert and Turner [1972] who point out the dangers of applying small-scale microstructure laboratory experiments to the larger medium-scale oceanographic case.

The second cause of fine structure: turbulence created by shear instability or the breaking of internal waves, billow turbulence, has been discussed by many, particularly by Woods and Wiley [1972], demonstrated in the laboratory by Thorpe [1969], and in the ocean thermocline off Malta by Woods [1968]. On an STD record one can easily find S-shaped profiles and mixed layers characteristic of billow turbulence, but these predominate at the higher wave numbers at scales of 1 m or less, which cannot be resolved with respect to density. At larger scales, S-shaped profiles are invariably statically stable and clearly are not billows. Both these mechanisms — double diffusion and billow turbulence — which really belong to the true microstructure scale involve some degree of vertical mixing. When we look at the medium-scale structure there is nothing to suggest that the numerous irregularities in the profiles are direct expressions of the vertical mixing. The features are well stratified, density-compensating and aligned

along isopycnal surface, all of which points to horizontal advection. This view seems to have gained universal acceptance. Stommel and Federov [1967] produced simple models to illustrate how the interleaving could arise and Stern [1969], showed that a horizontal variation in T & S could give rise to layered convection.

Although it is easy to see how, for example, the extensive mixing in the Strait of Gibraltar and along the continental shelf and slopes of the Spanish and Portuguese coasts could provide a ready source of different water types, there still remain some problems to be resolved e.g., the life time of an inversion layer of thickness ΔZ is given by

$$T = \frac{(\Delta Z)^2}{8\ K_z} .$$

If we accept that $K_z \sim 1$ cm^2/s the current value required by most thermocline models and also the value estimated by Munk [1966] for the deep ocean, then for, say, a 20 m thick inversion, T works out at about 6 days. Yet we still find pronounced medium-scale structure 500 miles away from the source of mixing where the travel time must be at least several months. We therefore conclude that either the interleaving must be a continuing process that is active away from the source, or the value for K_z must be much smaller. To attempt to answer this question we need to look at the interchange taking place at the interfaces, i.e. we need to examine the microstructure.

However, before I move on to discuss the microscale, there is one important aspect of fine-scale stratification that must be mentioned as it is a possible manifestation of double diffusion. In the boundary zones of larger-scale water masses there is often a tendency toward the formation of step layers. Sometimes we find a spectacular series of steps, as shown in Fig. 5, which in this case are associated with the lower boundary layer of the Mediterranean water.

I first observed this structure in 1966. This picture dates from a later cruise in 1969 [Tait and Howe (1970)]. Similar observations have been made by Johannessen and Lee [1974] and by Molcard [1975] in the Tyrrhenian Sea, by Neshyba [1969] in the Arctic Ocean, and Lambert [1975] in the W. Atlantic. The steps here average about 20 m in thickness for the mixed layer and 7 m for the interface. The mean T & S interface increments are as shown. Higher-resolution traces in Figs. 6 and 7 give the profile in more detail.

We have shown that these layers can extend for up to 30 miles and over this distance the mean T of a mixed layer varies by only a few hundreds of a Celsius degree. The system is stable; the steps are density compensating, with T exerting sufficient control to maintain stability.

Elliott has shown that the life time of a step layer is given by $\frac{(\Delta z)^2}{80\ K_z}$, i.e. one tenth that of an inversion layer (this is assuming that a layer once formed is allowed to diffuse away). My observations have shown no significant change in the system over two to three weeks. Molcard [1975] has recently produced impressive evidence that the Tyrrhenian Sea layer system has a life-time that must be reckoned in terms of years. One can only conclude from this that steady-state conditions prevail and that the interfaces are maintained by convection within the mixed layer.

All this is in accordance with double-diffusion theory, in particular the salt-finger case that is applicable here. Turner has demonstrated how a series of convecting layers can be established by salt fingering. If salt fingering is going to occur in the ocean then it is at interfaces such as this where we are most likely to find it and recently Williams [1974], using an optical technique, and Magnell [1975] using a towed sensor, have demonstrated the existence of salt fingers both in the Mediterranean outflow region and also in the Tyrrhenian sea steps. The salt-finger theory, when combined with the oceanographic data, enables us to calculate the heat and salt flux through the steps and arrive at values of about 1 cm^2/s for Ks and about 0.6 cm^2/s for Kt. However, theory and observation are not quite in accordance regarding the depth dimensions of the layers but the answer to this may again be in the microstructure of the interfaces. Recent work with high resolution probes has shown the interfaces to possess their own step structure, which is more in line with the theoretical scale predictions.

3. MICROSCALE PHENOMENA

The STD systems left us with much data but few answers and it was felt that the key to the whole vertical mixing process would be in the microstructure range from 1 m to 1 cm. We needed to examine the microscale density structure for evidence of shear instabilities and of double-diffusive effects and to determine the relative roles of these two mixing processes in the ocean. The study of the fine-scale structures had given the impression of a lamina as opposed to a turbulent ocean. Some degree of turbulence must however be associated with local mixing at interfaces and boundaries.

In an attempt to gain insight into the physical processes taking place at the interface areas, users of standard STD systems pushed the resolution to the limit. Dissatisfaction with what could be achieved led to the development of what I have already referred to as the new generation instruments — the true microstructure recorders — which began to appear around 1970 and are still being developed.

Two types of instruments evolved: the free-fall self-recording type, as described by Gregg and Cox [1971], and the more traditional suspended type, such as the Niel Brown CTD. Both these instruments are capable of resolving centimetre-scale fluctuations.

Measurements with the Cox free-fall probe have been extensively discussed by Osborne and Cox [1972], Gregg and Cox [1972], Gregg, Cox and Hacker [1974], and Gregg [1975]. I have time to review only the most important aspects of this work, starting with Osborne and Cox [1972], who in a key paper laid down some basic ideas, that have had a considerable influence on subsequent work. Taking as their model a laterally-homogeneous ocean and assuming steady-state conditions they derived an expression relating the turbulent heat flow to the microscale temperature fluctuations.

They showed that the ratio of the temperature gradient variance to the square of the mean gradient is related to the actual rate of diffusion of heat relative to that which would occur due to molecular diffusion along the mean gradients. By this means they arrived at an expression for K_z:

$$K_z = k \cdot \frac{(\nabla\theta')^2}{(\nabla\bar{\theta})^2} = k \cdot C$$

where $\theta_z = \theta'_z + \bar{\theta}_z$.

The ratio $\frac{(\nabla\theta')^2}{(\nabla\bar{\theta})^2}$, which subsequently became known as the Cox number, C, in an expression of the degree of microstructure present. We thus have a means of estimating K_z from the microstructure measurements. In evaluating K_z in this manner one must assume that the temperature gradient variance measured is representative of the oceanic area in which one is working and also that there is no net lateral transport of temperature fluctuations into the region. The validity of these assumptions is still in question and a wide range of K_z values have been obtained using this technique.

The Gregg and Cox MSR (microstructure recorder) measured the temperature gradient directly as well as the temperature and conductivity profiles. In a subsequent paper, Gregg and Cox [1972] discuss a single profile taken with this instrument in the San Diego trough (Fig. 8).

The T & S points are averaged over 20 cm: it is not a full resolution record. What is striking here is the general similarity between this picture and the fine-scale Mediterranean outflow records. We have a similar situation in the presence of two water types, in this case the lower-salinity northern water and the more saline water from the south. The stability is expressed here in terms of the square of the Väisälä frequency averaged over 84 cm on the left and 5 m on the right. On the smaller scale some instabilities involving about 8% of the profile are indicated associated with the features marked AD & E, but otherwise the stable structures can be assigned to the lateral advective process.

The T/S diagram in Fig. 9 could well be a NE Atlantic T/S diagram, except for the different scale. The instability at A is obvious while those at D & E appear as loops in the T/S trace.

The high-resolution profile enables us to look at these regions in detail: e.g. Fig. 10 shows the region around feature A in Fig. 8 at a resolution of 0.36 cm. The N^2 profile is given at resolution of 2.9 cm and 84 cm.

Some degree of small-scale overturn resulting from shear instability is suggested by the high level of activity associated with the density inversion, but the picture is inconclusive. More definite evidence of billow turbulence is shown in Fig. 11. Here we have the gradient profile on the left and the temperature on the right showing a characteristic 1 m scale overturn. Gregg and Cox conclude that about 1% to 2% of any record in the area have signatures suggestive of local overturning.

On the other hand, examination at high resolution of the larger stable inversions showed that the interfaces could be resolved into several sharp steps strongly suggestive of layering produced by double-diffusive phenomena. An example is shown in Fig. 12.

Some of these are very sharp (< 2 cm in thickness). Heat flux calculations showed general agreement with measured fluxes from the laboratory experiments on double diffusion. The authors thus find evidence in the microstructure for both processes: shear instability and double diffusion. They finally apply the Osborne and Cox equation to different parts of the record and obtain values of $K_z \sim \frac{1}{2} - 1$ cm^2/s for the most active regions and 0.02 cm^2/s for the relatively "quiet" sections.

Subsequent to this work in the San Diego trough, the next observations reported were from a contrasting site, hopefully typical of mid-ocean conditions, in the centre of the sub-tropical gyre in the North Pacific [Gregg, Cox, and Hacker (1973)]. The discussion in this paper centres on the gradient spectra. Back in 1968 Roden [1968] had described STD profiles in terms of wave number spectra and this theme was taken up by several other investigators. The problem was complicated by the need to remove the overall trend in the records before spectral analysis, and results obtained were much influenced by the type of filter used. With gradient spectra this difficulty largely disappears and we have the added advantage of dealing directly with the gradient variance, which, as we have seen, is a direct expression of the microstructure.

Compared with previous near-shore records, the mid-ocean data show a distinct lack of features on the medium scale. Activity was also generally low on the microscale. A section of one record (Fig. 13) did however show a step structure of the salt fingering type.

Figure 14 shows the measured T gradient, which reveals the structure of the interfaces (high gradient) region and the mixed layers. The wing thermistor, which describes a helical path as the instrument rotates during descent, covers a distance ten time greater than that of the nose probe. In spite of this low angle of attack (6°) little additional structure is seen, which implies that the structures are horizontal. Unfortunately the detection of centimetre-scale salt fingers is beyond the cutoff of the wing probe.

4. MICROSTRUCTURE SPECTRA

Figure 15 shows a composite gradient spectra built up from STD records for the low wave numbers ($K = 2 \times 10^{-3} - 2 \times 10^{-1}$ cycle/m), from the gross temperature data for $1 \times 10^{-2} - 6$ cycle/m from the gradient measurements for 1×10^{-1} to 6×10^{1} cycle/m. The spectra divide into two groups, shallow and deep, covering the range 200 to 2000 m. Although the variance spectrum levels vary appreciably by a factor of 100 from shallow water to deep, the ratio of the variances to the squares of the mean gradients shows a range of less than two. This means that the normalized microstructure levels are uniformly low. The Cox number is about 2, which yields a vertical thermal diffusion coefficient of $K_z = 3 \times 10^{-3}$ cm^2/s i.e. little above the molecular value.

This is in marked contrast to the situation near shore, where we had a value of 3.7×10^{-1}. In spite of the fact that the mean temperature gradient at the Pacific site is twice that in the San Diego trough, the spectral levels are lower at all wave numbers and by a factor of more than 50 in the microstructure range. All this points to the conclusion that the velocity shears, which generate the microstructure, must be much weaker at the mid-ocean site.

In a recent paper, Gregg [1975] discusses two profiles from stations about 10 km SW of Cabo San Lucas in the California current (Fig. 16). Although separated by only a few kilometres, these stations present quite different structures: one is similar to the mid-gyre records with an irregular "steppy" appearance and a low Cox number, while the other, which shows much activity on both medium and microstructure scales, has a large average Cox number. The first type is considered to represent the background condition of the ocean in which the levels of vertical turbulence are quite low and the principal dissipation occurs by small-scale instabilities at the step structures. The second type, characterized by the presence of appreciable medium-scale structure (due to multiple interleaving of different water types) has regions of intense microstructure activity, associated with the intrusion interfaces, which is considered to result from shear and double-diffusive effects. The San Diego trough records belong to this class.

The high microstructure levels associated with temperature inversions indicate that they are major factors in the dissipation of temperature and salinity fluctuations. While inversions occur on many

vertical scales, the observations suggest that it is the ones from several metres to a few tens of metres that produce the particularly high levels of microstructure. The oceanic regions with high dissipation rates can therefore be identified from standard STD profiles. Some of these regions are reasonably well known already but much can still be learnt from STD work.

The microstructure observations have done much to identify some of the small-scale mixing processes and have given some estimates of vertical heat fluxes, rate of energy dissipation, etc. What is required for the future is associated measurements of current shear in order to determine the Richardson number on the microscale. Instruments for this purpose are being developed: Simpson [1972], Osborne [1974]. This will lead to more reliable estimates of the energy dissipation rate, ϵ, a factor of great importance in ocean physics.

All the evidence to date points toward high rates of energy exchange occurring in sporadic bursts in specific regions in an otherwise quiet ocean. The key to the active areas lies in the juxtaposition of different water masses where the presence of an appreciable fine-scale structure is a likely indicator of regions of increased acoustic variability.

REFERENCES

BETHELL, J.P. The fine structure of the ocean, SACLANTCEN TM-184. La Spezia, Italy, SACLANT ASW Research Centre, 1972. [AD 753 445].

COOPER, L.H.N. Stratification in the deep ocean. Science Progress 55, 1967: 73-90.

COOPER, J.W. and STOMMEL, H. Regularly-spaced steps in the main thermocline near Bermuda. Jnl of Geophysical Research 73, 1968: 5849-54.

GILMOUR, A.E. Temperature stratification in the western Mediterranean Sea. Deep Sea Research 19, 1972: 341-353.

GREGG, M.C. and COX, C.S. Measurements of the oceanic microstructure of temperature and electrical conductivity. Deep Sea Research 18, 1971: 925-934.

GREGG, M.C. and COX, C.S. The vertical microstructure of temperature and salinity. Deep Sea Research 19, 1972: 355-376.

GREGG, M.C. The microstructure of the ocean. Scientific American 228 (2), 1973: 65-77.

GREGG, M.C., COX, C.S. and HACKER, P.W. Vertical microstructure measurements in the central North Pacific. Jnl of Physical Oceanography 3, 1973: 458-469.

GREGG, M.C. Microstructure and intrusion in the California Current. Jnl of Physical Oceanography 5, 1975: 253-278.

HAMON, B.V. Medium-scale temperature and salinity structure in the upper 1500 m in the Indian Ocean. Deep Sea Research 14, 1967: 169-181.

HOWE, M.R. and TAIT, R.I. Further observations of the thermohaline stratification in the deep ocean. Deep Sea Research 17, 1970: 963-972.

HOWE, M.R., ABDULLAH, M.I. and DEETAE, S. An interpretation of the double T-S maxima in the Mediterranean outflow using chemical tracers. Jnl of Marine Research 32, 1974: 377-386.

HUPPERT, H.E. and TURNER. J.S. Double-diffusive convection and its implication for the temperature and salinity structure of the ocean and Lake Vanda. Jnl of Physical Oceanography 2, 1972: 456-461.

ICHIYE, T. and SUDO, H. Saline deep water in the Caribbean Sea and in the Gulf of Mexico, Ref 71-16-T. College Station, Texas, Texas A & M University, 1971.

JOHANNESSEN, O.M. and LEE, O.S. Thermohaline staircase structure in the Tyrrhenian Sea. Deep Sea Research 21, 1974: 629-639.

KATZ, E.J. Diffusion of the core of Mediterranean water above the Mid-Atlantic Ridge crest. Deep Sea Research 16, 1970: 275-295.

LAMBERT, R.B. Graduate School of Oceanography, Univ. of Rhode Island, Kingston, R.I. Private communication.

LINDEN, P.F. On the structure of salt fingers. Deep Sea Research 20, 1973: 325-340.

MADELAIN, F. Influence de la topographie du fond sur l'écoulement Mediterranéen entre le détroit de Gibraltar et le Cap Saint-Vincent. Cahiers Oceanographiques 22, 1970: 43-62.

MaGNELL, B.A., EG & G Inc. Environmental Consultants Div., Waltham, Mass. 02154. Private communication.

MOLCARD, R. and WILLIAMS, A.J. Deep stepped structure in the Tyrrhenian Sea. Mémoires Société Royale des Sciences de Liège 6 (7), 1975: 191-210.

MUNK, W. Abyssal recipes. Deep Sea Research 13, 1966: 707-730.

NEAL, V.T., NESHYBA, S. and DENNER, W. Thermal stratification in the Arctic Ocean. Science 166, 1969: 373-374.

OSBORNE, T.R. and COX, C.S. Oceanic fine structure. Geophysical Fluid Dynamics 3, 1972: 321-345.

OSBORNE, T.R. Vertical profiling of velocity microstructure. Jnl of Physical Oceanography 4, 1974: 109-115.

PINGREE, R.D. Small-scale structure of temperature and salinity near St Cavall. Deep Sea Research 16, 1969: 275-295.

PINGREE, R.D. In situ measurements of salinity, conductivity and temperature. Deep Sea Research 17, 1970: 603-610.

PINGREE, R.D. Analysis of the temperature and salinity structure in the region of Mediterranean influence in the N.E. Atlantic. Deep Sea Research 18, 1971: 841-844.

STERN, M.E. and TURNER, J.S. Salt fingers and convecting layers. Deep Sea Research 16, 1969: 497-511.

SIEDLER, G. Die Haufigkeitsverteilung von Wasserarten in Ausstromgebiet von Meeresstrassen. Kieler Meeresforschungen 24, 1968: 59-65.

SIMPSON, J.H. A free-fall probe for the measurement of velocity microstructure. Deep Sea Research 19, 1972: 331-336.

TAIT, R.I. and HOWE, M.R. Some observations of thermohaline stratification in the deep ocean. Deep Sea Research 15, 1968: 275-280.

TAIT, R.I. and HOWE, M.R. Thermohaline staircase. Nature 231 (5299), 1971: 178-179.

THORPE, S.A. Experiments on the stability of stratified shear flows. Jnl of Fluid Mechanics 39, 1969: 25-28.

TURNER, J.S. and STOMMEL, H. A new case of convection in the presence of combined vertical salinity and temperature gradients. Proceedings National Academy of Science (U.S.) 52, 1964: 49-53.

TURNER, J.S. Salt fingers across a density interface. Deep Sea Research 14, 1967: 599-611.

TURNER, J.S. The influence of molecular diffusivity of turbulent entrainment across a density interface. Jnl of Fluid Mechanics 33, 1968: 639-656.

SHIRTCLIFFE, T.G.L. and TURNER, J.S. Observations of the cell structure of salt fingers. Jnl of Fluid Mechanics 41, 1970: 707-719.

WILLIAMS, A.J. Salt fingers observed in the Mediterranean outflow. Science 185, 1974: 941-943.

WOODS, J.D. Wave-induced shear instability in the summer thermocline. Jnl of Fluid Mechanics 32, 1968: 791-800.

WOODS, J.D. and WILEY, R.L. Billow turbulence and ocean microstructure. Deep Sea Research 19, 1972: 87-121.

ZENK, W. On the temperature and salinity structure of the Mediterranean water in the northeast Atlantic. Deep Sea Research 17, 1970: 627-631.

ZENK, W. On the Mediterranean outflow west of Gibraltar. METEOR Forschungsergebnisse Reihe A, 16, 1975: 23-34.

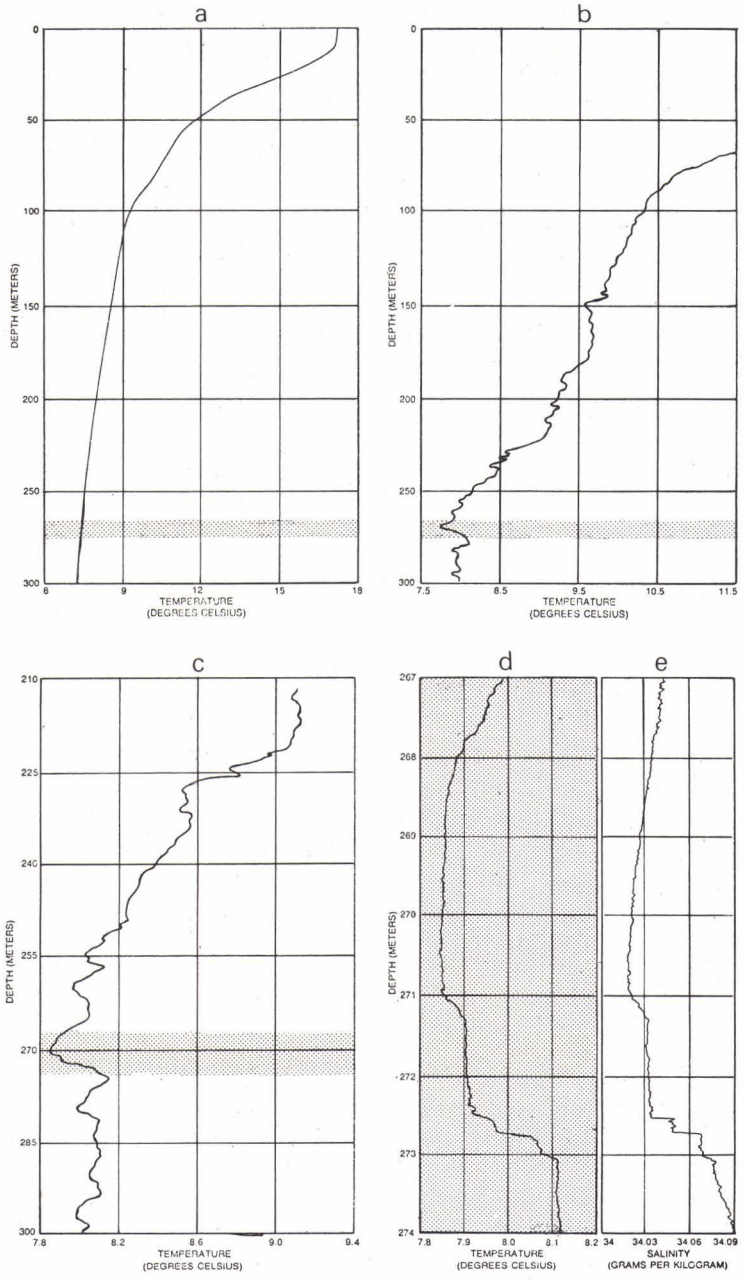

FIG. 1 TEMPERATURE PROFILES (GREGG 1973)

a. TEMPERATURE PROFILE FROM NANSEN CAST
b. STD RECORD OF THE SAME PROFILE
c. HIGHER RESOLUTION TRACE
d. CENTIMETRE SCALE RESOLUTION

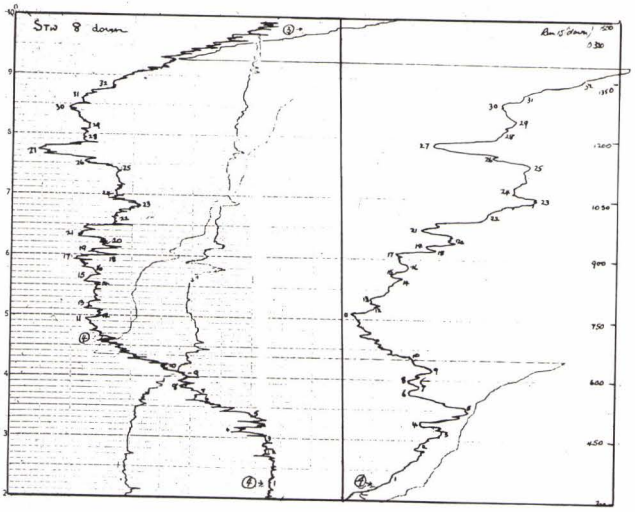

FIG. 2
STD RECORD. DISCOVERY 1966 STA. 8

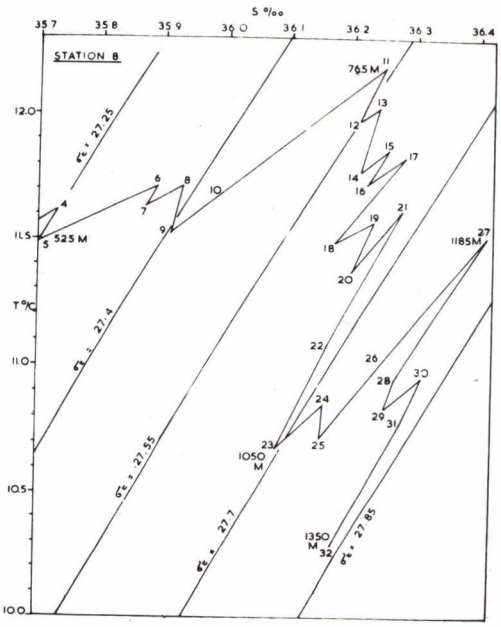

FIG. 3
T/S DIAGRAM. DISCOVERY 1966 STA. 8

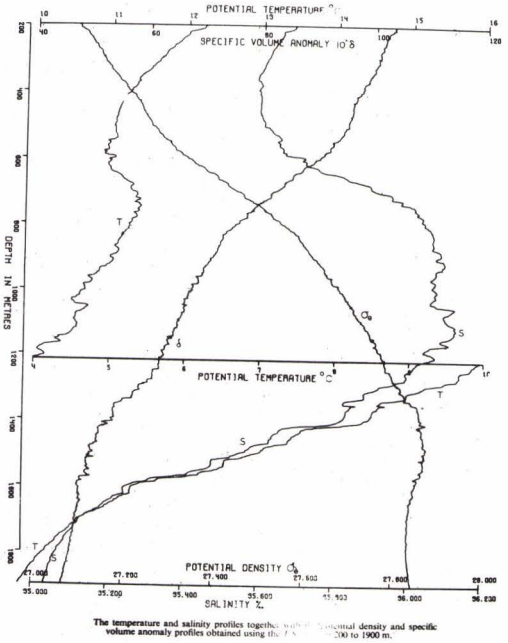

The temperature and salinity profiles together with potential density and specific volume anomaly profiles obtained using the [illegible] 200 to 1900 m.

FIG. 4
PROFILES OF T, S, σ_θ & δ (PINGREE, 1970)

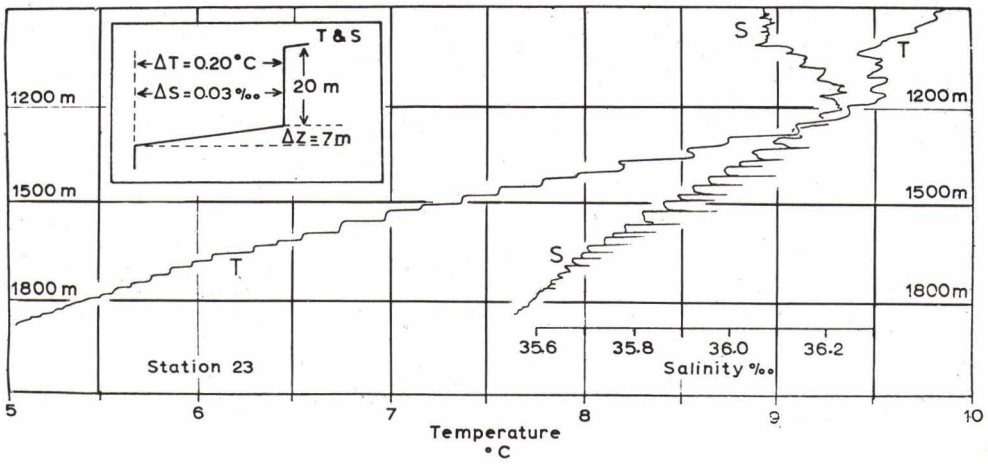

FIG. 5 THERMOHALINE STAIRCASE (TAIT & HOWE, 1970)

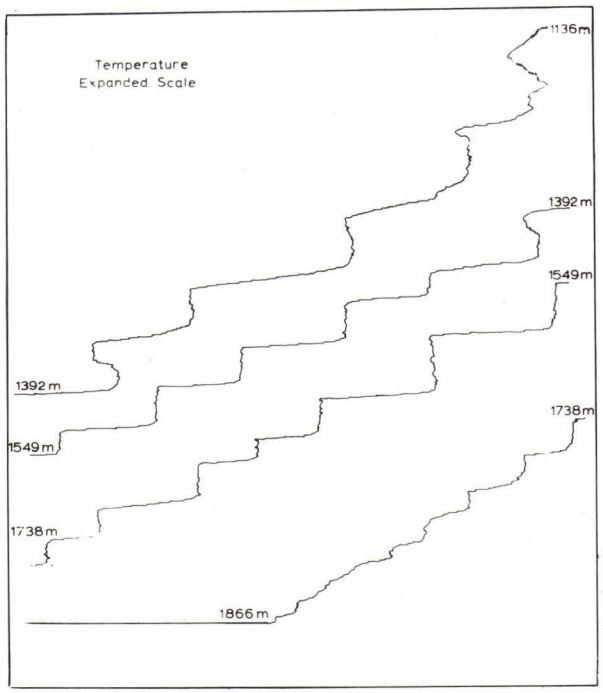

FIG. 6
EXPANDED SCALE RECORD STA. 23

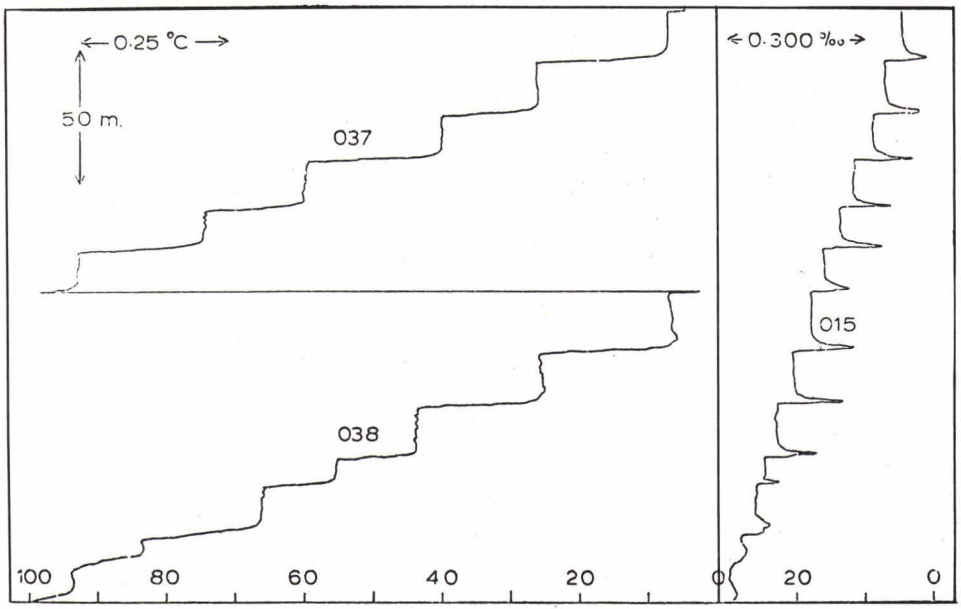

FIG. 7 EXPANDED SCALE RECORD STA. 28

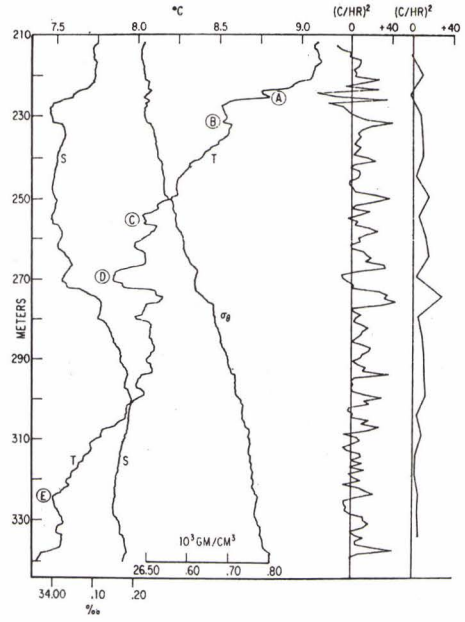

FIG. 8
MSR RECORD (GREGG & COX, 1972)

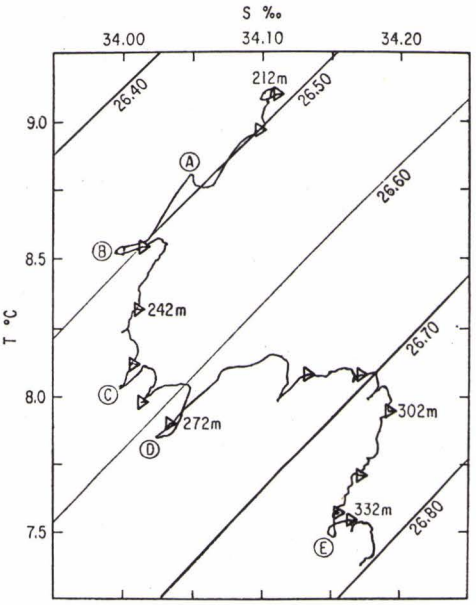

FIG. 9
T/S DIAGRAM (GREGG & COX, 1972)

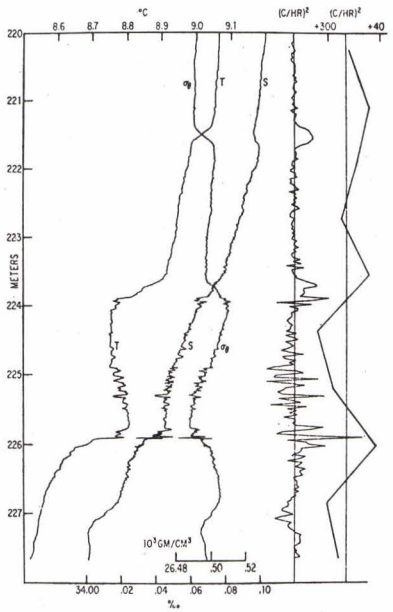

FIG. 10
MSR TRACE AT HIGH RESOLUTION (GREGG & COX, 1972)

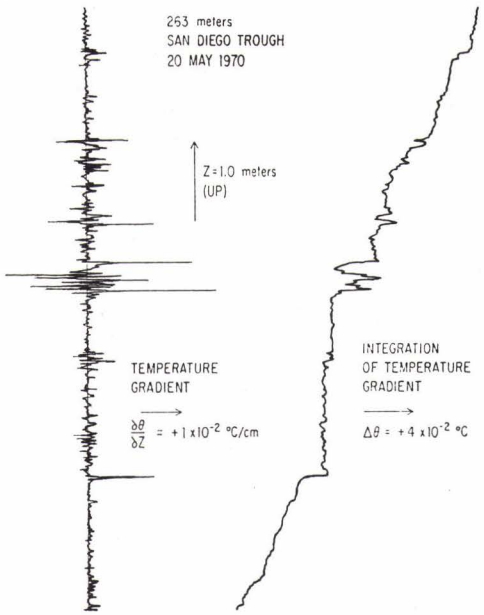

FIG. 11
HIGH RESOLUTION TEMPERATURE & TEMPERATURE GRADIENT PROFILE (GREGG & COX, 1972)

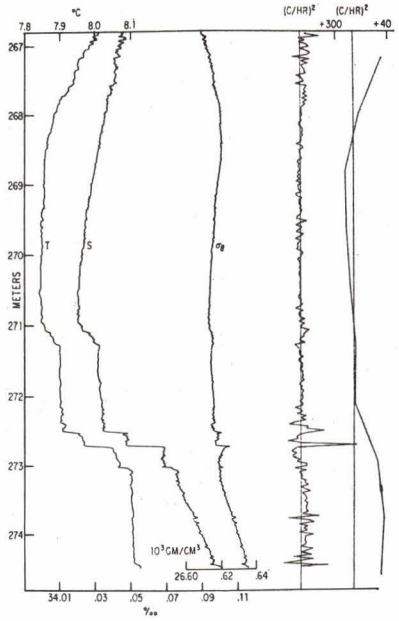

FIG. 12
MSR RESOLUTION OF INVERSION INTERFACE (GREGG & COX, 1972)

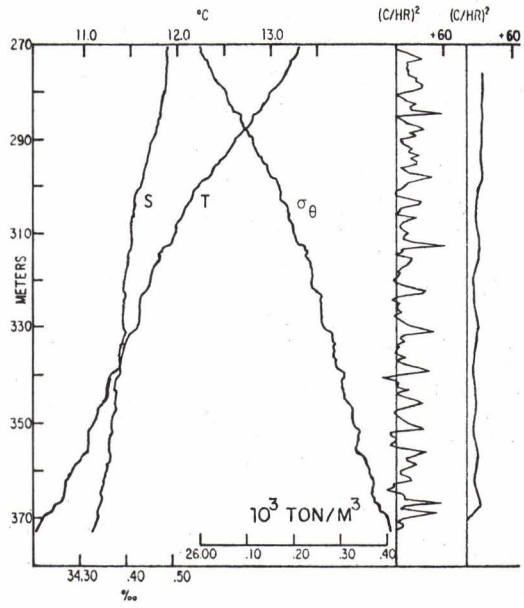

FIG. 13
MID-OCEAN STATION (GREGG, COX & HACKER, 1973)

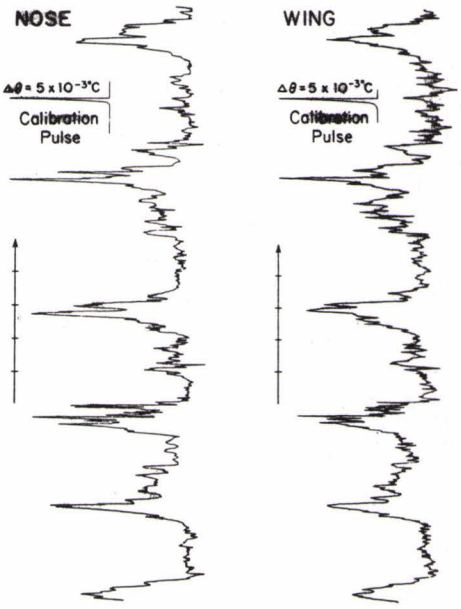

FIG. 14
TEMPERATURE GRADIENT PROFILES FOR STEP-LIKE STRUCTURES (GREGG, COX & HACKER, 1973)

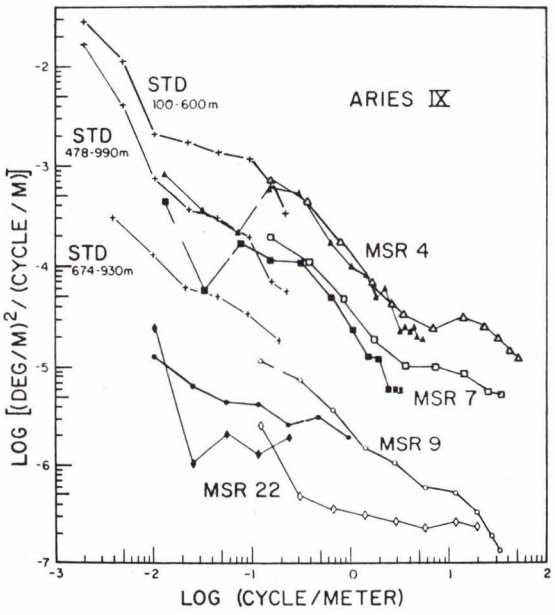

FIG. 15
GRADIENT SPECTRA – GREGG, COX & HACKER, 1973

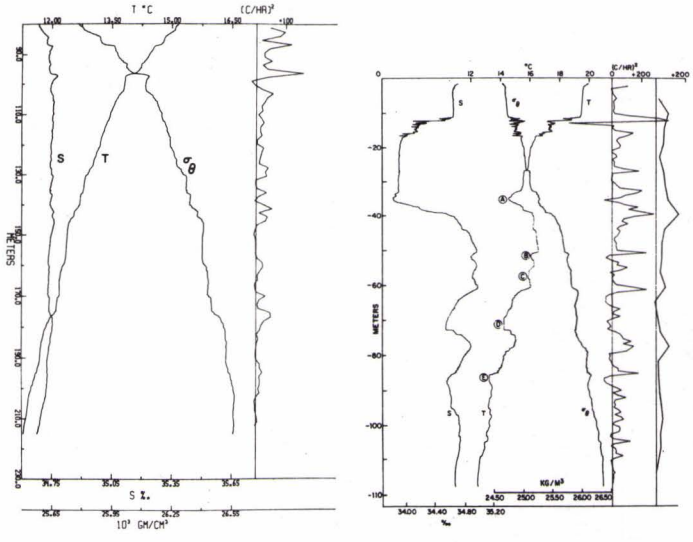

FIG. 16
MSR RECORDS SHOWING THE TWO GENERAL TYPES OF PROFILE

ACOUSTIC EFFECTS OF INTERNAL MICROSTRUCTURE

by

David Mintzer
Rebecca Crown Center and Technological Institute
Northwestern University
Evanston, Illinois 60201
U.S.A.

(No Abstract received)

Introduction

Since the purpose of this meeting is to promote the interaction of oceanographers and acousticians, I'm not going to talk about some of the very interesting mathematical problems that arise in the theory of the scattering of waves by a randomly-inhomogeneous medium: multiple scattering problems, the details of the controversy surrounding the Born and the Rytov method of approximately solving the wave equation, the question of gross inhomogeneities, etc. These are all quite interesting but, I believe, relatively unimportant in the context of oceanographic measurements and modelling. I will concentrate instead on the two sides of the single question of interest here: what does the microstructure of the ocean do to an acoustic wave traversing it, and what can measurements of acoustic waves tell us about the ocean microstructure. Much of our small successes in this field, as in other fields of physics, have come about

because of a suitably narrowly-defined area of interest.

In the first place, let me define the time scale. I am going to talk about oceanic phenomena whose time scale ranges from, say, tenths of a second to tens of seconds. Phenomena which might take place on a shorter time scale are simply averaged out in the process of sampling the data, as would be any "noise". Larger time scale "variations" introduce slow changes in time of the average values of the variables of interest, and can be ignored by defining averages local in time. Of course, if the "noise" or the "variations" have time scales which blend into the time scale of interest, then these phenomena cannot be ignored, but must be treated as part of the problem. The small end of the time scale helps define the frequency of the sound waves with which we wish to probe the ocean. We wish to have the acoustic wave period much smaller than the smallest oceanic time scale of interest so that a pulse consisting of a number of acoustic wave periods views each point of the ocean as time-independent.[1c] From the frequency domain point of view, scattering from a time-dependent phenomenon introduces broadening in the acoustic spectrum of the order of the frequency scale of the phenomenon. As long as the time scale we are

sampling is no shorter than, say tenths of a second, the broadening will be of the order of tens of hertz, and is unimportant. The long time scale effects can be separated out since the acoustic signals are normally pulsed to separate out boundary effects from the effects of the body of the medium; thus, moving averages can be easily handled. However, these are not trivial considerations, since the fact that we are treating statistical phenomena means that we must average over long time periods. The theory demands that the measurements sample the entire universe of statistical possibilities, so that the probability that a certain configuration of the medium occurs in nature is reflected in the same probability that it happens in the measurements. Phenomena which change in a time scale of tens of seconds must therefore be sampled over hundreds of seconds to be reasonably sure of having measured an unbiased universe. To be honest, I shouldn't say that we don't seem to have any time scale problems in the measurements, but rather that the crudeness of our measurements probably doesn't allow us to recognize any difficulties.

One can make similar comments about the size of the portion of ocean in which measurements are to be made. The shortest distance from source to receiver is determined,

aside from acoustic beam-forming considerations, by the desire to have a large sample of the universe of physical sizes involved in the measurements.[1a,2] In a sense, there is a certain competition between distance and time in the statistical character of the measurements, since physically one would expect that large-scale-in-space phenomena are associated with long times for significant changes. In looking for the effects of large physical sizes of inhomogeneities, it would appear necessary to do averaging over a long time interval. At the other end of the scale, the largest distance for measurements, from a practical point of view, is set by surface reflection interferences, and by gross inhomogeneities in the ocean.

I'd like to say a word now about laboratory experiments. In performing acoustic measurements on microstructure scattering in a laboratory, one is not trying to reproduce the ocean, but only to reproduce what are believed to be the important aspects of the natural phenomenon to be studied. Thus, if the theory and the laboratory experiments are in good agreement, then one should expect that natural phenomena which can be described in terms of the parameters important to the theory should also be in good agreement with the theoretical predictions. As I shall describe later, we

do find that the theoretical predictions concerning the statistics of the sound pressure fluctuations in an acoustic wave agree well with the measurements of such a wave traversing a tank of water heated from below.[3] The theory requires, as the important non-acoustic factor, that the scalar sound speed is a random function of space and time with certain known averages. We may confidently expect that we may use this technique in the ocean and correctly determine certain statistical parameters of the ocean microstructure - if this is the predominent phenomenon. If the speed of sound in the ocean is changing slightly in a random manner (with appropriate time and space scales) due, for example, to changes in temperature or salinity, then we may expect the theory to give correct results. However, if the sound speed changes because the hero of "Jaws" appears on the scene, then the theory is useless. I have stressed this because of two reasons. It has been suggested that the simple idea that the microstructure is due to the intermingling of slowly moving blobs of warm or cool water is incorrect, but that it is due to a turbulent spectrum[4,5] rather than a Gaussian one. If the idea here is that the sound-speed variations are due to temperature variations carried along by a turbulent mixing

process, then this change makes no difference to the basic theory, which is given in terms of the microstructure correlation function of the scalar sound speed; anything that affects the scalar sound speed is fair game for the theory. However, if the turbulent mixing is presumed so strong that the change in the local sound speed is due to the actual motion of the water, then the theory cannot be applied because it is developed for a scalar variation, not the vector variation that a fluid velocity would introduce. From measurements in the ocean, the root-mean-square temperature variations producing acoustic fluctuation effects are of the order of $0.02^{\circ}C$; corresponding fluid velocity variations would have to be of the order of 10 cm per second to give acoustic effects of the same order of magnitude. A second point to be noted is that it has been suggested that bubbles might be the cause of acoustic fluctuations.[6] The work, by Professor Medwin, assumes that the scalar sound-speed changes due to changes in the compressibility of the air-water mixture with the random fluctuations coming from fluctuations in the number of bubbles per unit volume or in the resonant frequencies of the bubbles. Again, here the acoustic wave sees an effect of a change in scalar sound speed, and the theory is applicable. In short, one cannot apply the theory without

thought as to the assumptions. Differences between theoretical expectations and experimental results may be simply due to incorrectly assumed parameters, such as a wrong form for the refractive index correlation function; or it may be due to the invalidity of the theory, caused by applying it to the wrong physical situation. However, when applicable, I believe that the theory is sufficiently well proven to allow acoustic measurements to be useful as a probe for the measurement of ocean microstructure.

The final point I wish to make in this Introduction, concerns modelling - the topic of this conference. There are many good things to be said about modelling, but there is one very important point to remember, especially when modelling statistical phenomena, where the measurements are, of necessity, incomplete. The point not too often stressed is -- don't take the models too seriously. The ocean is a complex medium, and models, to be useful, tend to simplify -- be prepared to abandon a model if the experimental results so demand. Remember that the model is not the phenomenon; it is a substitute for the phenomenon.

General formulation[1,5,7]

Consider an unbounded medium with a sound speed which changes randomly with position and time only slightly from its mean value; the refractive index is:

$$\frac{c_0}{c(\underline{r},t)} = 1 + \alpha\, n(\underline{r},t)\ ;\ \langle n\rangle = 0\ ;\ \langle n^2\rangle = 1 \qquad (1)$$

We have chosen c_0 as an appropriate average sound speed, and α is simply a size parameter. The average to be taken (angular brackets) is as a long-time average at any point; by the assumption of statistical homogeneity, this is the same as an average taken over all of space at one instant of time; it may also be looked upon as an average taken over the ensemble of all distributions of refractive index variations. If the acoustic pulse passes any point in space in a time small compared to the characteristic time of change of the refractive index at a point, we may neglect the time-dependence of the refractive index.[1a,c] Each pulse thus traverses a different distribution of refractive index variations, so that a suitably large number of pulses samples the entire ensemble.

We may write the wave equation for the acoustic pressure, to first order in α, under these conditions:

$$\nabla^2 p(\underline{r}) + k_0^2 \left[1 + \alpha\, n(\underline{r})\right] p(\underline{r}) = 0\ ;\ k_0 = \frac{\omega}{c_0} \qquad (2)$$

We shall describe the pressure in terms of its amplitude and phase:

$$p(\underset{\sim}{x}) = |p(\underset{\sim}{x})| \; e^{i S(\underset{\sim}{x})} \tag{3}$$

There are two separate parts of the problem to be concerned with: the statistical aspect and the inhomogeneity aspect. The statistical aspect means that we must describe the pressure in terms of averages, deviations from the mean, and so forth. The quantities we shall work with are the simplest ones: the deviation from the mean of the pressure amplitude, non-dimensionalized by the mean value; and the deviation from the mean of the phase:

$$\delta P(\underset{\sim}{x}) = \frac{1}{\langle |p| \rangle} \left[|p| - \langle |p| \rangle \right] \; ; \; \delta S(\underset{\sim}{x}) = S - \langle S \rangle \tag{4}$$

From these quantities we may form coefficients of variation, two-point correlation functions, etc.

$$V_{pp}^2 = \langle \delta P(\underset{\sim}{x}) \, \delta P(\underset{\sim}{x}) \rangle \quad ; \quad V_{ss}^2 = \langle \delta S(\underset{\sim}{x}) \delta S(\underset{\sim}{x}) \rangle \tag{5}$$

$$\Pi_{pp}(\underset{\sim}{x}_1, \underset{\sim}{x}_2) = \left[V_{pp}(\underset{\sim}{x}_1) \, V_{pp}(\underset{\sim}{x}_2) \right]^{-1} \langle \delta P(\underset{\sim}{x}_1) \, \delta P(\underset{\sim}{x}_2) \rangle \tag{6}$$

The inhomogeneity problem comes about because we can't solve the wave equation exactly for a general refractive index; in fact, we can't even solve it exactly for practically

any refractive index. Two approximation techniques have been used, the Born or single-scattering approximation, and the Rytov approximation. For our purposes, where we will work only to first order in α, we needn't concern ourselves with the difference, but it is of significance for higher-order approximations. I should note that I originally thought that the Born approximation had as large a region of validity as that of Rytov, although some people claimed that Rytov was better. I now suspect that the Rytov approximation is the better one; in fact, I'm writing a paper illustrating that it is so — although these statements are certain to start an argument in some quarters! However, I must admit that I don't know why the Rytov approximation has a larger region of validity, and that bothers me.

If we solve the wave equation to first order in α, using the single-scattering approximation, we may write for the acoustic pressure

$$p(\underset{\sim}{r}) = \frac{e^{ik_0 r}}{r} + \frac{k_0^2 \alpha}{2\pi} \int n(\underset{\sim}{r}') \frac{e^{ik_0|\underset{\sim}{r}-\underset{\sim}{r}'|}}{|\underset{\sim}{r}-\underset{\sim}{r}'|} \frac{e^{ik_0 r'}}{r'} d\underset{\sim}{r}' \qquad (7)$$

We find, therefore, as might be expected:

$$\langle |p| \rangle = \frac{1}{r} \quad ; \quad \langle S \rangle = k_0 r \qquad (8)$$

One may solve for the deviations from the mean, most simply written in terms of prolate spheroidal coordinates:

$$\delta P = (k_0^2 \alpha r^2/4\pi) \int d\underset{\sim}{\xi}' \; n(\underset{\sim}{\xi}') \; \cos[k_0 r(\xi'-1)] \qquad (9)$$

$$\delta S = (k_0^2 \alpha r^2/4\pi) \int d\underset{\sim}{\xi}' \; n(\underset{\sim}{\xi}') \; \sin[k_0 r(\xi'-1)] \qquad (10)$$

These results involve no approximations other than the stated ones: scalar sound-speed variations, single scattering, and the characteristic time for change in the refractive index small compared to the pulse length.

The statistics of the medium are described in terms of the refractive index variation average (of zero), mean-square average (of α^2) and its correlation function:

$$N(\underset{\sim}{r}'-\underset{\sim}{r}'') = N(x'-x'', y'-y'', z'-z'') = \langle n(x', y', z') \, n(x'', y'', z'') \rangle \qquad (11)$$

$$\mathcal{N}(\underset{\sim}{k}) = \frac{1}{(2\pi)^{3/2}} \int d\underset{\sim}{r} \; N(\underset{\sim}{r}) \; e^{i\underset{\sim}{k}\cdot\underset{\sim}{r}} \qquad (12)$$

Isotropic case:

$$N(\underset{\sim}{r}) = N(r) \quad ; \quad \mathcal{N}(\underset{\sim}{k}) = \mathcal{N}(k) \; ; \quad \Phi(k) = 4\pi k^2 \mathcal{N}(k) \qquad (13)$$

where $\mathcal{N}(\underset{\sim}{k})$ is the Fourier transform of the correlation function, and $\Phi(k)$ is the spectral density of the refractive index correlation. I will not restrict myself to the isotropic case until later. Since δP and δS are in terms of the refractive index variations at an arbitrary

point, the coefficients of variation and the two-point acoustic correlation will involve averages over products of these variations, that is, the refractive index correlation function. By various devious methods, one may carry out some of the integrations, and transform others into looking relatively harmless; under the condition $k_o r >> 1$, we obtain what might be considered the general form for the coefficients of variation:

$$V_{pp}^2 = (8\pi\sqrt{2\pi})^{-1} \alpha^2 k_o^2 r^2 \int d\underset{\sim}{k}\, \mathcal{N}(\underset{\sim}{k}) \int_0^{\pi} \sin\theta' d\theta' \int_0^{\pi} \sin\theta'' d\theta'' \tag{14}$$

$$\times \exp\left[\tfrac{1}{2} i k r \cos\theta (\cos\theta' - \cos\theta'')\right] \sin\left[\frac{k^2 r}{8k_o} \sin\theta'\right] \sin\left[\frac{k^2 r}{8k_o} \sin\theta''\right]$$

The results for V_{ss} , the coefficient of variation of the phase, is the same, except for the substitution of $\cos\left[\frac{k^2 r}{8k_o} \sin\theta'\right]$, etc., at the end of the integral. These results are valid under the previously mentioned physical conditions (scalar variations, single-scattering, appropriate time scale), and $k_o r >> 1$; the single-scattering approximation may be written as $\alpha^2 k_o^2 a r << 1$, where a is a characteristic size parameter of the refractive-index correlation function. The models which can be developed are all to be contained in the form of the correlation function, $N(\underset{\sim}{r})$, or its Fourier transform, $\mathcal{N}(\underset{\sim}{k})$.

Results of approximations

I will now only talk about the amplitude fluctuations, although similar comments can be made about the phase fluctuations. Under the condition that $r/k_o a^2 \ll 1$, we see that $k^2 r/8k_o$ is small for all relevant values of k, and the sines may be approximated by their arguments. This is the high-frequency approximation, or the ray limit. If $r/k_o a^2 \gg 1$, we may make some transformations to a somewhat different form, which can also be approximated, although the results are different for the cases of $k_o a \gg 1$ and $k_o a \ll 1$, that is, for the characteristic length parameter of the correlation function large or small as compared to the sound wavelength. The usual condition is that the correlation length is large compared to the wavelength. The limiting cases are[1a,b,8]

$$V_{pp}^2 = \frac{1}{60}\alpha^2 r^3 \int_0^{\infty} \nabla^2 \nabla^2 N(\rho)\, d\rho \quad ; \quad r/k_o a^2 \ll 1 \qquad (15)$$

$$V_{pp}^2 = \alpha^2 k_o^2 r \int_0^{\infty} N(\rho)\, d\rho \quad ; \quad r/k_o a^2 \gg 1 \qquad (16)$$

$$k_o r \gg 1 \; ; \; \alpha^2 k_o^2 a r \ll 1 \; ; \; k_o a \gg 1 \; ; \; r/a \gg 1$$

The arrow on the integral sign denotes that the integration

is taken along the line from source to receiver. If the correlation function is not isotropic, the integration brings in different characteristic lengths depending upon the orientation of the principal axes of the correlation function with respect to the source-to-receiver line. This will be illustrated later.

The interpretation of these results is well known. In the ray theory, the change in intensity in going a short distance along the ray path is proportional to the relative change in the cross-sectional area of a bundle of rays. The cross-sectional change is proportional to the Laplacian of the refractive index, which then gives rise to the form in the ray limit. In the diffraction limit, on the other hand, it is the constructive and destructive interference between scattered waves which causes the sound pressure variations. Such interference depends upon the relative path lengths traversed by the waves, and thus directly upon the path integral over the refractive index variations. In the cases shown here, we are in the limit of $k_o a \gg 1$; since the scattering angle of a wave impinging upon an obstacle of size a is $\theta \approx 1/k_o a$, the scattering angle is small and the predominant effect occurs due to waves scattered along the line from source to receiver. In the

case of small $k_c a$, the form for the coefficient of variation is quite different, but leads to a smaller value than for the large $k_c a$ case.

The first question one might ask is whether or not the theory and the experiments agree. The answer is not to be looked for, I believe, in ocean experiments because they are simply "not clean": there is usually source and receiver motion, gross inhomogeneities, probably inhomogeneous statistics, and so forth. The primary purpose of laboratory experiments, on the other hand, is simply to check out the theory, since a good laboratory experiment involves the measurement of all of the variables. I'll only use the prettiest slide of the Stone and Mintzer experiments[3c], showing the linearity with frequency of the coefficient of variation in the diffraction limit, and its independence of frequency in the ray limit; corresponding graphs of V vs. distance shows the appropriate square-root dependence and the 3/2 - power dependence for the two limiting regimes. It is, moreover, interesting to note that the acoustic data is internally consistant, even though the data was taken during many separate experiments run over a long period of time. This is to be expected, since the temperature

microstructure was formed by the same grid of heating wires each time, approximately the same power inputs were used, and the temperature of the surroundings was about the same; thus the same temperature structure for the body of water could be expected, at least in the statistical sense. Thus, the value for $\alpha a^{1/2}$, which is the combination of temperature microstructure parameters measurable by acoustic data in the diffraction limit, comes out to average $1.25 \times 10^{-4} \pm 2\%$ (cgs units) from a number of different experiments. Data from the ray limit gives closely similar values. Data taken from thermistor measurements of the temperature microstructure gives an $\alpha a^{1/2}$ value of slightly more than double that. Considering the fact that the experimentally-determined temperature microstructure correlation function is not truly Gaussian, and that the r.m.s. temperature microstructure experiments were very difficult to make, the agreement seems quite good. I must note that these data were taken during the Dark Ages, with the received acoustic pulses photographed from an oscilloscope trace and measured by hand and the thermistor readings also recorded by hand from a digital voltmeter, and the analyses all done on an electric desk calculator. With modern electronic equipment, PDP-8's, tape recorders and digital computers, we could have

INITIAL DISTRIBUTION

	Copies
MINISTRIES OF DEFENCE	
MOD Belgium	1
DND Canada	10
CHOD Denmark	8
MOD France	8
MOD Germany	15
MOD Greece	11
MOD Italy	10
MOD Netherlands	12
CHOD Norway	10
MOD Portugal	5
MOD Turkey	5
MOD U.K.	16
SECDEF U.S.	60
NATO AUTHORITIES	
Defence Planning Committee	3
NAMILCOM	2
SACLANT	10
SACLANTREPEUR	1
CINCWESTLANT/COMOCEANLANT	1
COMIBERLANT	1
CINCEASTLANT	1
COMSUBACLANT	1
COMCANLANT	1
COMMAIREASTLANT	1
COMNORLANT	1
SACEUR	2
CINCNORTH	1
CINCSOUTH	1
COMNAVSOUTH	1
COMSTRIKFORSOUTH	1
COMEDCENT	1
COMSUBMED	1
COMMARAIRMED	1
CINCHAN	1

	Copies
SCNR FOR SACLANTCEN	
SCNR Belgium	1
SCNR Canada	1
SCNR Denmark	1
SCNR Germany	1
SCNR Greece	1
SCNR Italy	1
SCNR Netherlands	1
SCNR Norway	1
SCNR Portugal	1
SCNR Turkey	1
SCNR U.K.	1
SCNR U.S.	2
NATIONAL LIAISON OFFICERS	
NLO Denmark	1
NLO Italy	1
NLO U.K.	1
NLO U.S.	1
NLR TO SACLANT	
NLR Belgium	1
NLR Canada	1
NLR Germany	1
NLR Greece	1
NLR Italy	1
NLR Norway	1
NLR Portugal	1
NLR Turkey	1
ESRO/ELDO Doc. Service	1
ATTENDEES	110